Universidade do Minho
Escola de Medicina

Jorge Carlos Dias de Sousa Filho

Fluorescent tag *Sporothrix brasiliensis*: a tool for host-pathogen interaction studies

outubro de 2022

Fluorescent tag *Sporothrix brasiliensis*: a tool for host-pathogen interaction studies
Jorge Carlos Dias de Sousa Filho
UMinho | 2022

Universidade do Minho
Escola de Medicina

Jorge Carlos Dias de Sousa Filho

Fluorescent tag *Sporothrix brasiliensis*: a tool for host-pathogen interaction studies

Dissertação de Mestrado
Mestrado em Ciências da Saúde

Trabalho efetuado sob a orientação de
Doutor Fernando José Santos Rodrigues
e de
Doutor Ricardo Jorge Leal Silvestre

outubro de 2022

DIREITOS DE AUTOR E CONDIÇÕES DE UTILIZAÇÃO DO TRABALHO POR TERCEIROS

Este é um trabalho académico que pode ser utilizado por terceiros desde que respeitadas as regras e boas práticas internacionalmente aceites, no que concerne aos direitos de autor e direitos conexos.

Assim, o presente trabalho pode ser utilizado nos termos previstos na licença abaixo indicada.

Caso o utilizador necessite de permissão para poder fazer um uso do trabalho em condições não previstas no licenciamento indicado, deverá contactar o autor, através do RepositóriUM da Universidade do Minho.

Licença concedida aos utilizadores deste trabalho

Atribuição-NãoComercial-SemDerivações
CC BY-NC-ND

https://creativecommons.org/licenses/by-nc-nd/4.0/

Agradecimentos

Aos meus orientadores, Doutor Fernando Rodrigues e Doutor Ricardo Silvestre, pela orientação e pela oportunidade de poder aprender convosco e pelos inúmeros ensinamentos que muito contribuíram para o meu crescimento profissional e pessoal.

À doutora Cristina Cunha, pela orientação, ajuda disponibilizada e pelos inúmeros ensinamentos que muito contribuíram para o meu crescimento profissional e pessoal.

Ao Relber Gonçalves e Ana Frias, grandes amigos e brilhantes pesquisadores que doaram seu tempo, suor e sangue para a realização de diversos experimentos realizados na construção dessa tese. Sem vocês dois, certamente a conclusão dessa difícil etapa seria impossível.

A Daniela Antunes, Rita Gomes e demais pesquisadores que me disponibilizaram imenso apoio científico e ajuda pessoal. Esta jornada foi seguramente mais fácil graças a vocês.

Ao Ehsan, Sara, Sônia, Stephanie, Consuello, Ian, Cláudio entre diversos outros pesquisadores com quem desenvolvi uma amizade no laboratório, ajudando a tornar todo o processo menos difícil.

Agradeço ao ICVS – Instituto de Ciências da Vida e Saúde pela oportunidade e experiência. E também a Fundação para a Ciência e a Tecnologia pelo apoio financeiro dado a esse estudo - FCT-2022.03348.PTDC - Sporob_SiA: Elucidation of the role of sialidase 1 in the severity of feline sporotrichosis caused by Sporothrix brasiliensis.

E por último, mas não menos importante, à minha família. Aos meus pais, tia e meu namorado, pessoas indispensáveis ao longo da minha trajetória. Tudo o que alcancei se deve a vocês. Serei eternamente grato por todas as oportunidades que me concederam, todo o afeto e por todos os esforços e sacrifícios que fizeram por mim ao longo do caminho.

STATEMENT OF INTEGRITY

I hereby declare having conducted this academic work with integrity. I confirm that I have not used plagiarism or any form of undue use of information or falsification of results along the process leading to its elaboration.

I further declare that I have fully acknowledged the Code of Ethical Conduct of the University of Minho.

Fluorescent tag *Sporothrix brasiliensis*: a tool for host-pathogen interaction studies

Abstract

Sporotrichosis is considered an emerging health problem, being the world's most prevalent subcutaneous mycosis, occurring on mammal hosts, which facilitates zoonotic transmission. *Agrobacterium tumefaciens*-mediated transformation (ATMT) is a broadly technique used for both plants and fungus transformation. Here, we report the establishing of an ATMT system for *S. brasiliensis*, considering different strains of *A. tumefaciens* and *S. brasiliensis* and several conditions of co-cultivation. Our results point to 72h of co-cultivation at 26°C, the AGL-1 bacterial strain, and the 2:1 ratio (bacteria:fungi) as ideal conditions for a high number of transformants. In these conditions, we obtained 3179 ± 1171 mutants/co-cultivation. PCR analysis showed that all Hygromycin B resistant clones tested harboured a copy of the *HPH* gene. FACS analysis showed high mitotic stability of the GFP gene in pGAPDH::GFP mutants. The *S. brasiliensis* pGAPDH::GFP and pGAPDH::H2A::GFP strains were respectively used to evaluate the phagocytosis index and fungicidal activity,. pGAPDH::GFP cytoplasm expression of GFP allowed a strong fluorescence visualization inside monocytes/macrophages in both microscopic and FACS analysis. The phagocytosis index was 64.25 ± 9.96% at the MOI of one peripheral blood mononuclear cell (PBMC) to five pGAPDH::GFP yeast cells, with two hours of infection. The pGAPDH::H2A::GFP *S. brasiliensis* strain failed to provide a correlation between loss of fungal viability or fungal death and loss of GFP fluorescence in all fungicidal experiments performed. Furthermore, its GFP fluorescence was not visible upon monocytes/macrophages engulfment in both microscopic and FACS analysis. Our results showed, firstly, an efficient genetic toolbox to create large-scale transformant libraries for *S. brasiliensis,* and secondly, the possibility to use the pGAPDH::GFP strain in phagocytosis assays without fluorophore stain prior to infection. Together, these results can help provide new insights to better understand the host-pathogen interactions and virulence mechanism for the *Sporothrix* spp..

Keywords: ATMT, fluorescent tag strains, sporotrichosis, *Sporothrix brasiliensis*.

Marcadores fluorescentes em *Sporothrix brasiliensis*: uma ferramenta para estudos de interação entre hospedeiro e patógeno

Resumo

A esporotricose é um problema de saúde emergente e a micose subcutânea mais prevalente no mundo. Esta doença ocorre em hospedeiros mamíferos, o que facilita a sua transmissão zoonótica. A transformação mediada por *Agrobacterium tumefaciens* (ATMT) é uma técnica amplamente utilizada para a transformação de plantas e fungos. No presente trabalho, estabelecemos um sistema de ATMT para *S. brasiliensis*, considerando diferentes estirpes de *A. tumefaciens* e *S. brasiliensis,* bem como várias condições de co-cultivo. Os nossos resultados apontam para 72h de co-cultivo a 26°C, a estirpe bacteriana AGL-1 e o rácio de 2:1 (bactérias:fungos) como condições ideais para a obtenção de um elevado número de transformantes. Nestas condições, obtivemos 3179 ± 1171 transformantes/co-cultivo. A análise de RT-*PCR* demostrou a presença de uma cópia do gene *HPH*. A análise de FACS mostrou alta estabilidade mitótica do gene GFP dos isolados da estirpe pGAPDH::GFP. Os mutantes pGAPDH::GFP e pGAPDH::H2A::GFP de *S. brasiliensis* foram respetivamente usados para calcular o índice de fagocitose e a atividade fungicida. A expressão citoplasmática de GFP da estirpe de pGAPDH::GFP permitiu uma forte visualização de fluorescência dentro dos monócitos/macrófagos em análises de microscópica e FACS. Relativamente aos mutantes pGAPDH::H2A::GFP *S. brasiliensis* não foi possível obter uma correlação entre a perda de viabilidade fúngica ou morte fúngica e a perda de fluorescência GFP em todos as experiências realizadas no que diz respeito à avaliação da capacidade fungicida dos monócitos/macrófagos. Para além disso, não foi possível detetar a sua fluorescência GFP após ter sido fagocitado pelos monócitos/macrófagos em análises de microscópica e FACS. Em primeiro lugar, este trabalho permitiu a criação de uma ferramenta genética eficiente para construir bibliotecas de transformantes em larga escala para *S. brasiliensis*. Em segundo lugar, os nossos resultados demostraram que o mutante pGAPDH::GFP pode ser usado em ensaios de fagocitose sem a necessidade de coloração com fluoróforo antes da infeção. Em soma, os nossos resultados podem ajudar a entender melhor as interações hospedeiro-patógeno e o mecanismo de virulência da Sporothrix spp..

Palavras-chaves: ATMT, esporotricose, marcadores fluorescentes, *Sporothrix brasiliensis.*

Table of Contents

List of abbreviations

% – Percentage

°C – Degree Celsius

AIDS – acquired immunodeficiency syndrome

AS – Acetosyringone

ATMT – *Agrobacterium tumefaciens*-mediated transformation

BMDM – Bone marrow-derived macrophage

BSA – Bovine serum albumin

CD – Cluster of differentiation

cDMEM – Complete Dulbecco's modified Eagle's medium

CE – Chlorimuron ethyl

CE^{R} – Chlorimuron ethyl resistant

CO_2 – Carbon dioxide

cRPMI – Complete Roswell Park Memorial Institute Medium

CW – Cell wall

CFW – Calcofluor-white

DAMP – Damage-associated molecular pattern

DAPI – 4',6-Diamidino-2-Phenylindole, Dihydrochloride

DPBS – Dulbecco's phosphate-buffered saline

EDTA – Ethylenediaminetetraacetic acid

ELISA – Enzyme-Linked Immunosorbent Assay

FACS – Fluorescence-activated cell sorting

FCS – Fetal bovine serum

FITC – Fluorescein isothiocyanate

FSC – Forward scatter

GAPDH – Glyceraldehyde-3-phosphate dehydrogenase

GFP – Green Fluorescent Protein

GM-CSF – Granulocyte-macrophage colony stimulating factor

h – Hour

hMDM – Human monocyte-derived macrophages

HEPES – 4-(2-hydroxyethyl)-1-piperazineethanesulfonic acid

HPH – Hygromycin B phosphotransferase

HygB – Hygromycin B

HygB^{R} – Hygromycin B resistant

IL – Interleukin

IM – Induction medium

$KHCO_3$ – Potassium bicarbonate

L – Litre

LC-MS – Liquid Chromatography-Mass Spectrometry

M – Molar

MFI – Mean fluorescence intensity

mg – Milligram

min – Minutes

mL – Millilitre

mM – Millimolar

MACS – Magnetic-activated cell sorting

M-CSF – macrophage colony stimulating factor

MOI – Multiplicity of infection

NaCl – Sodium chloride

NH_4Cl – Ammonium chloride

ng – Nanogram

nm – Nanometre

OD – Optic density

PAMP – Pathogen-associated molecular pattern

PBMCs – Human peripheral blood mononuclear cells

PBS – Phosphate buffered saline

PCR – Polymerase chain reaction

pH – potential of hydrogen

PI – Propidium iodide

RNS – Reactive nitrogen species

ROS – Reactive oxygen species

rpm – Rotation per minute

RT – Room temperature

SDS – Sodium dodecyl sulfate

SEM – Standard error of mean

SSC – Side scattered

TE – Transposable elements

Th – T helper

Ti – Tumor inducing

TLR – Toll-like receptor

Tris-HCL – Tris(hydroxymethyl)aminomethane hydrochloride

UV – Ultraviolet

vir – Virulence

vol – Volume

YNB – Yeast nitrogen base medium

YPD – Yeast extract peptone dextrose medium

µg – Microgram

µL – Microliter

List of figures

List of tables

CHAPTER 1

Introduction

Sporotrichosis is the most prevalent subcutaneous mycosis worldwide and has become a public health concern that will likely worsen in the future (1). It is an acute or chronic granulomatous mycosis with wide geographic distribution, whose incidence and etiological agent vary according to geographic region, mostly based on case report observations (2). The etiologic agents of this disease are fungi often present in the pathogenic clade of the *Sporothrix* genus, but some cases can be caused by the environmental clade, associated with the sapronoses form of sporotrichosis (1,3). Among the *Sporothrix* genus, *S. brasiliensis* is reported to be the most virulent, exhibiting the worst clinical manifestations (4,5). Although sporotrichosis etiological agents have a susceptible response profile to antifungal drugs, several reports of drug resistance have already been recently reported (6,7). Nowadays Rio de Janeiro state in Brazil is the greatest feline zoonotic transmission epicentre, with more than 4,000 human and 4,000 feline diagnosed cases (8). Similar epidemics are also occurring in São Paulo and Rio Grande do Sul states, with a high prevalence of *S. brasiliensis* infections (5). Cats play an important role in the *S. brasiliensis* infection, due to their susceptibility to sporotrichosis and highly transmissibility to both felines and humans (9,10). Despite the increasing incidence of sporotrichosis, it is unclear which virulence traits are involved in the establishment, development, and severity of this disease.

1.1. *Sporothrix-schenckii* complex and sporotrichosis

Sporotrichosis was firstly reported in 1898 by the medical student Benjamin Schenck (11), and nowadays is the world's most prevalent and dispersed subcutaneous mycosis (12), being able to affect both immunodeficient (13) and immunocompetent hosts (14). Although inhalation of conidia can be a source of infection, humans are usually infected when the fungi reach subcutaneous tissue through a skin trauma, either by contaminated plant material or through the bites or scratches of cats with sporotrichosis (6). It is a subacute or chronic infection, which promotes a skin lesion at the inoculation site, resulting in an ulcerated nodule. Through the lymphatic system, the infection eventually spreads to other host organs, causing a more severe and disseminated version of the disease (15).

The sporotrichosis etiological agents belong to the *Sporothrix schenckii* complex (12), characterized by several ascomycetous thermally dimorphic fungi from the genus *Sporothrix* inside the Ophiostomatales order (16). As illustrated in Figure 1, they grow as cigar-shaped yeast-like cells at 37◦C or while infecting mammals and grow as sessile dematiaceous conidia along with hyaline sympodial conidia in its filamentous form at 25◦C or in the environment in substrates like living and decaying vegetation, animal excreta, and soil (2,5). Even though organisms that are part of the Ophiostomatales

order are normally associated with a plant or insect lifestyle, the *Sporothrix genus* exhibits pathogenicity to mammals. The mechanisms responsible for this are still poorly described (5).

These fungi are abundant in soil, wood, and moss, reaching mammals through skin lesion inoculation, a situation common to gardeners and farmers (12,17). After traumatic inoculation, the fungi transition to the parasitic yeast form. How efficient this morphological transition occurs and consequently the fungi pathogenicity varies accordingly to the *Sporothrix* species (5,17,18).

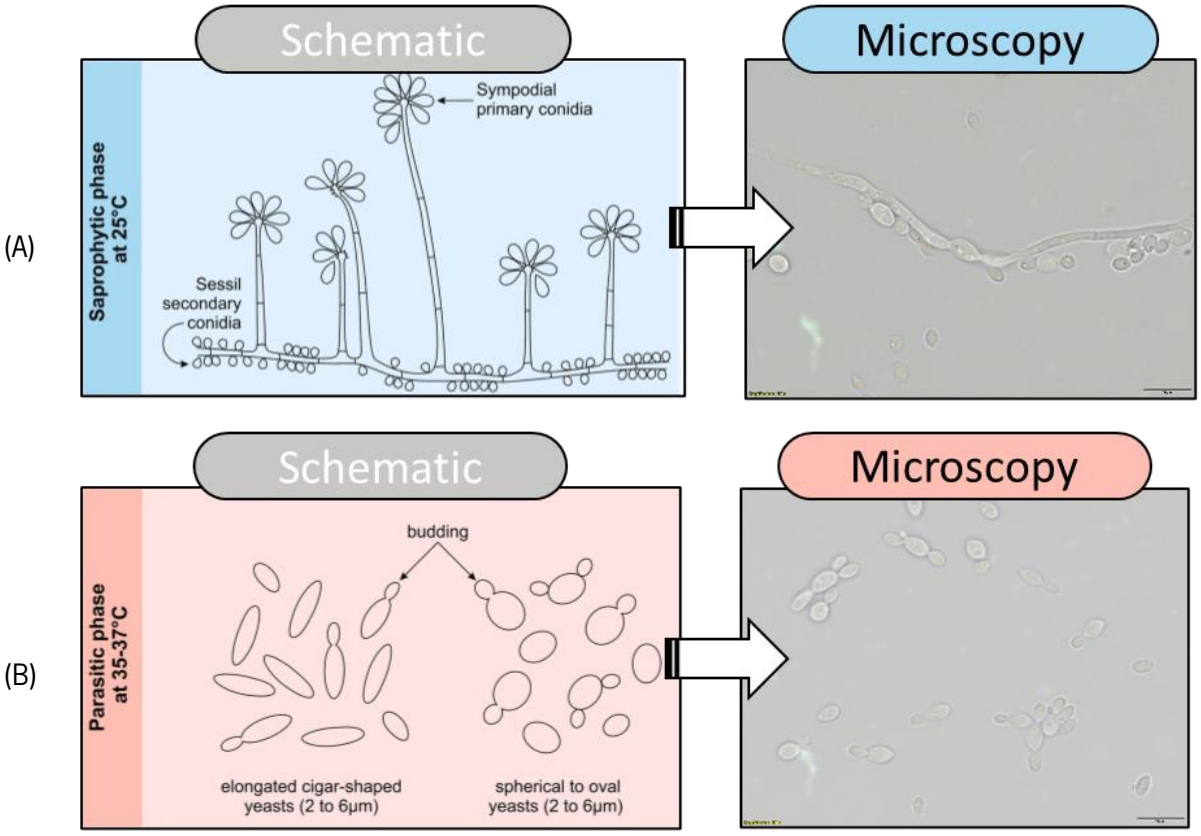

Figure 1. Thermal dimorphism morphology schematization and microscopic demonstration of *Sporothrix brasiliensis.* (A) Saprophytic morphology schematization and microscopic image. The scale bar equals 10µm. During the saprophytic (25-30°C) phase of *Sporothrix*, it develops septate hyaline hyphae with erect conidiophores. Two types of conidia are produced: the primary or sympodial conidia, with a hyaline thin wall, or the secondary or sessile conidia, with a thick wall of dark brown colour. **(B)** Parasitic morphology schematization and microscopic image. The scale bar equals 10µm. During the pathogenic/parasitic phase (35–37°C), morphology is characterized by oval or spherical yeasts (2–6µm), sometimes elongated in a cigar shape. Image adapted from Rodrigues et al., 2020.

Although sporotrichosis had been for an entire century exclusively attributed to the single species, *Sporothrix schenckii*, the development of advanced phylogenetic molecular techniques over the last decade allowed to address the role of other species such as *S. brasiliensis*, *S. globosa*, and *S. luriei*, *S. mexicana*, *S. pallida* and *S. schenckii stricto sensu*. This revolution highlighted significant differences in morphological, physiological, genetic, epidemiological, virulence traits and antifungal susceptibility among pathogenic *Sporothrix* spp (4,7,18–23). It elucidated that few of these *Sporothrix* species are successful mammal pathogens and therefore clinically relevant, such as *S. schenckii, S. brasiliensis, S. globosa*, and *S. luriei* (6,17,24).

Since a species complex is defined as a monophyletic clade of species with equivalent clinical relevance, the *S. schenckii* complex term has been classified as no longer appropriate. There is currently a suggestion to adopt the terms ''clinical clade'' or ''pathogenic clade'' to refer to *S. brasiliensis*, *S. schenckii*, *S. globosa* and *S. luriei*, species often isolated from human and animal cases, while the remaining *Sporothrix* species would be nested in an ''environmental clade,'' due to their often association with the sapronoses form of sporotrichosis (1,3).

Sporothrix spp. is strongly present in the genus Ophiostoma. Despite the members from this order are primarily associated with Protea or plant pathogens, *Sporothrix* spp. have never been observed as plant pathogens (25). They grow abundantly on dead wood, being omnipresent in the environment in dead wood, mosses, cornstalks, soil, and hay, and require a temperature of 22◦C–27◦C, 90% humidity, soil rich in cellulose and with a pH between 3.5 and 9.4 (25,26). Sporotrichosis is widely prevalent in warm-blooded animals and several mammals are prone to infection, such as humans, dogs, cats, rats, mice, chimpanzees, parrots, fishes, and dolphins (25,27). This large spectrum of hosts facilitates animal horizontal and zoonotic transmission of sporotrichosis (27). The route of infection varies with *Sporothrix* species. As illustrated in Figure 2, the species within *Sporothrix* environmental clade are generally associated with an environmental route of transmission, while the pathogenic clade, especially the *S. brasiliensis* species, is normally transmitted between infected animals where dissemination to humans can happen (1,5).

The human disease has a broad range of clinical manifestations and can be classified into fixed cutaneous, lymphocutaneous, disseminated cutaneous, and extracutaneous sporotrichosis (28). Cats are relevant zoonotic transmitters of sporotrichosis in Brazil and usually may present three clinical forms upon infection: cutaneous, lymphocutaneous, and disseminated (9). The cutaneous form is the most common, and ulcers are the main clinical signs observed (8). However, respiratory, ophthalmic, osteoarticular and central nervous system sporotrichosis infection and hypersensitivity reactions have

also been reported (12,27). Although in humans host immunodeficiency is often associated with the worst clinical presentations (12), such correlation has not been proven in felines yet (29,30).

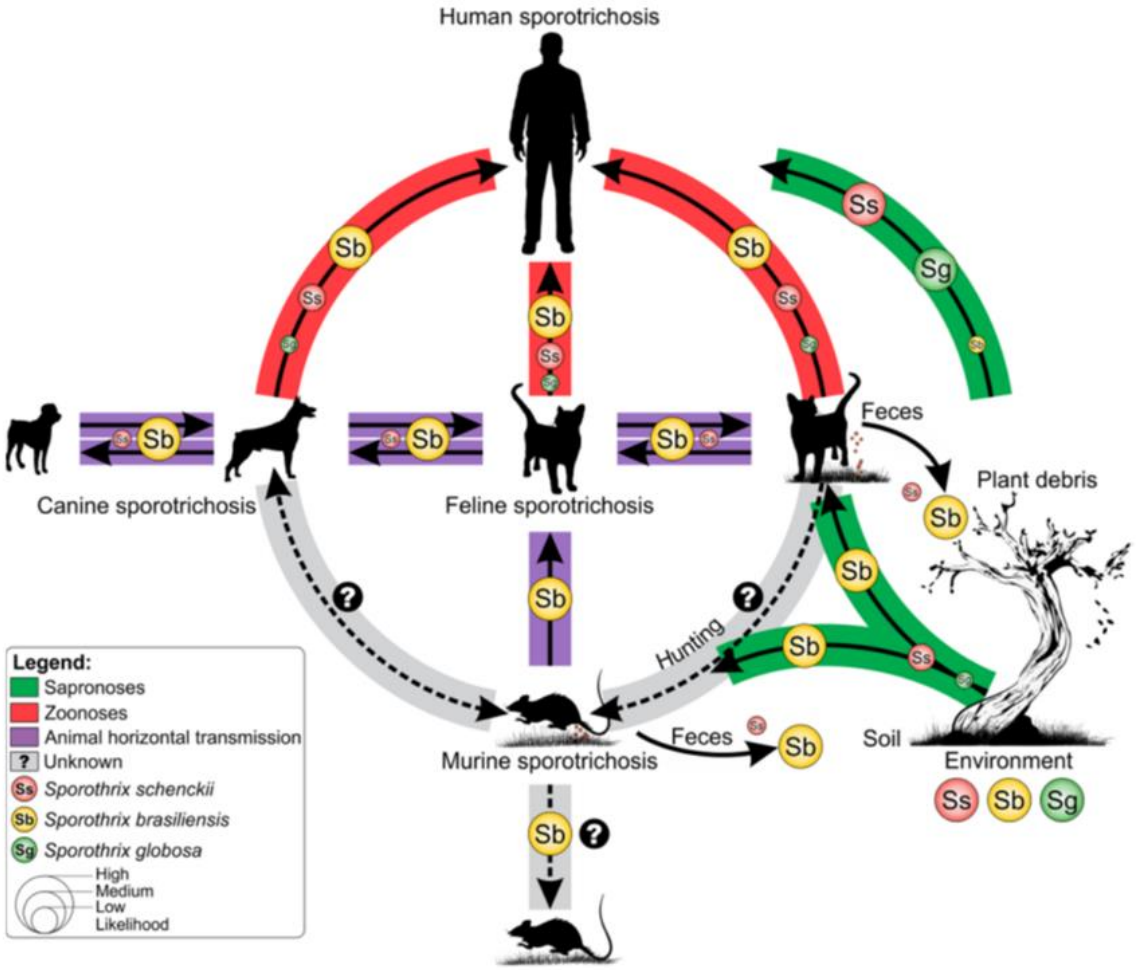

Figure 2. Transmission routes in human and animal sporotrichosis. The purple route (animal horizontal transmission) illustrates *S. brasiliensis* association with large epizooties during animal horizontal transmission. Although less frequent, the same route applies to *S. schenckii*. The zoonoses route (red) represents sporotrichosis which can be transmitted to humans via animal deep scratching and biting, especially from infected cats. Lastly, the green route (sapronoses) is associated with *S. schenckii* and *S. globosa* infections. The probability of involvement (high, medium, or low) is proportional to the size of the species' circumference in each transmission route. Image from Rodrigues et al., 2016.

1.2. Sporotrichosis epidemiological aspects

Although human sporotrichosis is generally responsive to standardized antifungal strategies, this disease is now considered an emerging health problem (8). Since sporotrichosis is not a reportable

disease, its exact prevalence is unknown (25), whereas the incidence is mostly based on case report documentation (2). As illustrated in Figure 3 and 4, this mycosis has wide geographic distribution and the etiological agent and disease burden vary from country to country and geographic region (2). It is estimated that in most regions of the world, more than 80% of cases are caused by a predominant species (1). In Asia, *S. globosa* counts for 99,3% of sporotrichosis cases and is a common subcutaneous infection in Japan, China, India, and Malaysia (1). In Australia and South Africa, it is estimated that *S. schenckii* has a predominance of 94%, while in south-eastern South America, *S. brasiliensis* is the etiological agent in 88% of cases. The case reports from sporotrichosis in humans in Africa still refer to sapronotic transmission, with some sporadic cases of infection in animals, despite the HIV/AIDS epidemic (1,31). Lastly, in western South America, Central and North America *S. schenckii* is the most predominant (89%), while *S. luriei* and *S. mexicana* are restricted to Africa and Mexico, respectively. (10,12,25,28). The disease is less prevalent in Europe, except for the unique outbreak that occurred in France, at the beginning of the nineteenth century (10,32).

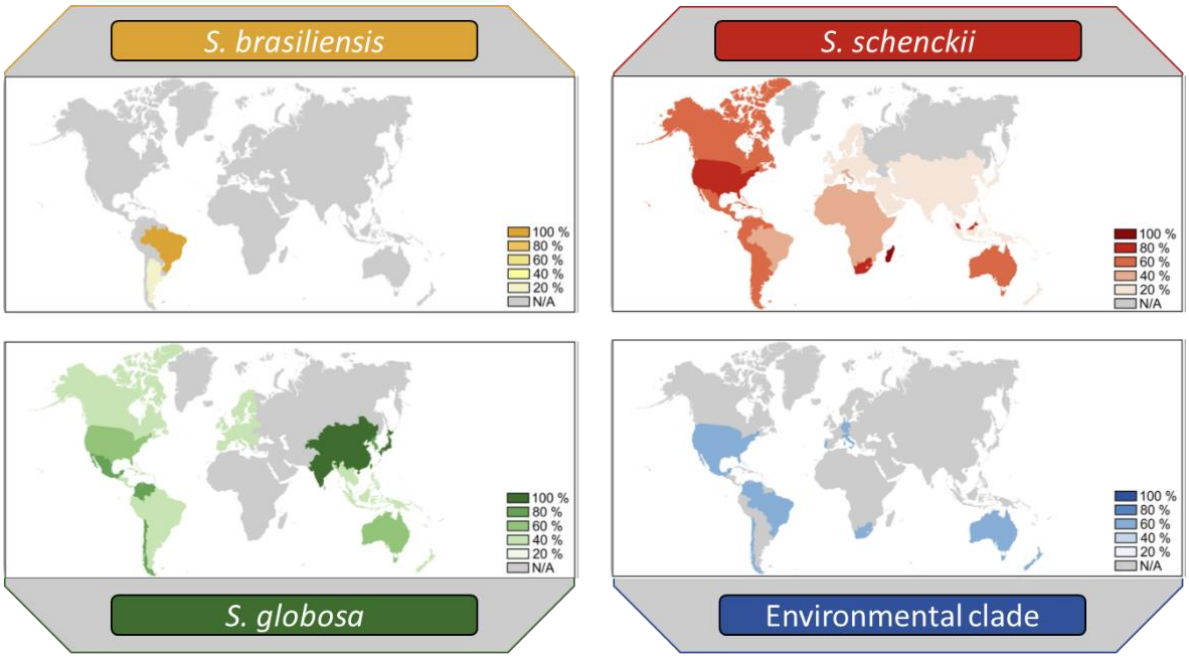

Figure 3. Recent global distribution of the species from the pathogenic (*S. brasiliensis*, *S. schenckii* and *S. globosa*) and the environmental clade of the *Sporothrix* species. *S schenckii* has almost worldwide distribution, while *S. brasiliensis* is restricted to the South and Southeast of Brazil. *S. globosa* is found less frequently in the Americas and Europe but is an emerging species in Asia. Sporotrichosis caused by the environmental clade is less frequent and spread worldwide. Image adapted from Rodrigues et al., 2020.

Figure 4. **Distribution and relative burden of sporotrichosis in the world.** Image from Chakrabarti et al., 2015.

Sporotrichosis is currently a hyperendemic disease in regions of countries like China, Mexico, Brazil, Peru, Venezuela, Colombia, and South Africa (1,10,12,27). For decades until the mid-1990s, feline sporotrichosis in Brazil appeared only as sporadic, self-limiting clusters. However, over the last decades in Brazil, the sporotrichosis epidemiological scenario changed drastically and became the most endemic country in the world (1,10). Clinical sporotrichosis in mammals results from two major infection routes: animal transmission and plant origin. Historically, sporotrichosis was a rare sapronoses (plant origin), caused by *S. schenckii* that present the classic and sporadic route of transmission by traumatic inoculation of the etiologic agent while handling organic matter, similar to the rest of the world. It was considered an occupational disease, occurring when workers are exposed to a high incidence of injuries with contaminated material (33). Nowadays, feline sporotrichosis caused by *S. brasiliensis* has led to a large epidemic with zoonotic transmission in Brazil, becoming the main etiological agent of feline and human sporotrichosis in the region (1,5,25,34).

Cats are very susceptible to sporotrichosis, and through deep scratching and biting, the disease is highly transmissible to both felines and humans, as an epizooty (cat-cat) and zoonosis (cat-human), respectively. Feline sporotrichosis challenging treatment, combined with the population's poor socioeconomic background and scarce access to human and veterinary health services are important factors that can explain the cause of this ongoing epidemic in Brazil (20,24,25).

Currently, cases of human sporotrichosis occur in 25 of the 26 Brazilian states. Zoonotic

sporotrichosis cases have been expanding rapidly toward the northeast regions of Brazil in recent years, which is directly linked to the feline sporotrichosis epizootic, as shown in Figure 5. This public health concern will likely worsen in the future since *S. brasiliensis* infection is projected to expand its biogeographic domains and host range and become more virulent (1).

Rio de Janeiro state is the greatest feline zoonotic transmission epicentre, with more than 4,000 human and 4,000 feline cases diagnosed at Fundação Oswaldo Cruz between 1998 and 2012 (8). Similar epidemics are occurring in São Paulo and Rio Grande do Sul states, also with a high prevalence of *S. brasiliensis* infections (5). Urban areas with high feline population densities seem to be important drivers of epizootics *S. brasiliensis* transmission, and the epidemiological profile group usually is people with poor socioeconomic conditions with direct and frequent contact with these animals, namely children, the elderly, and women. However, outside urban areas, the classical sapronoses transmission type prevails (5,35).

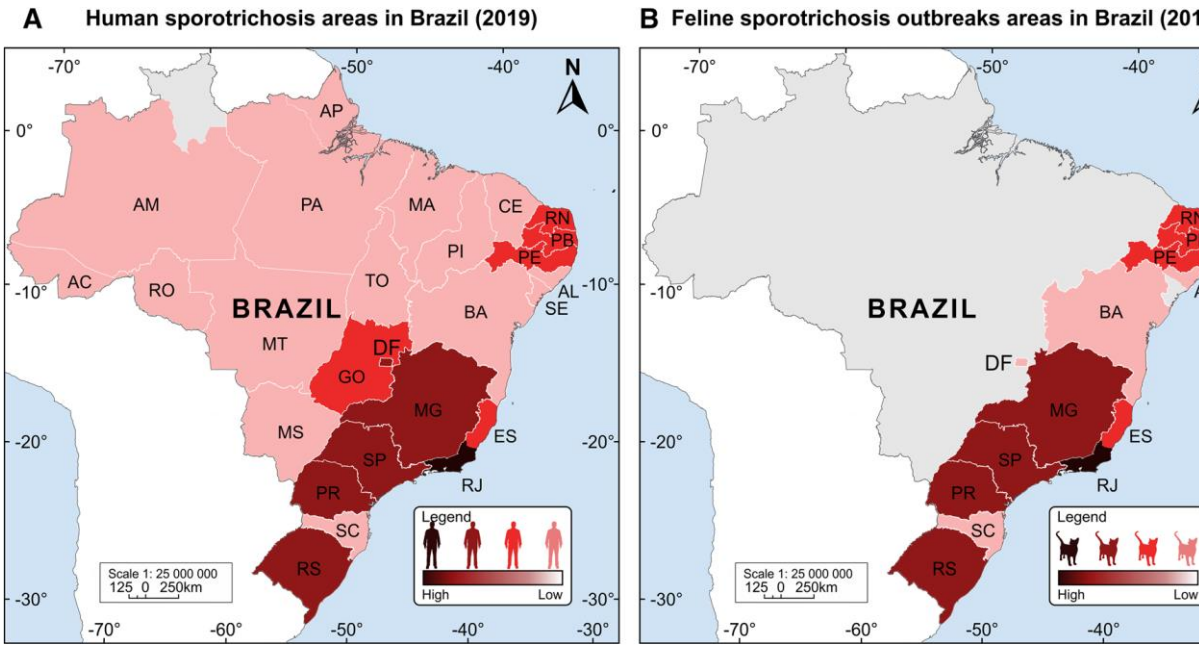

Figure 5. Geographic distribution of human and feline sporotrichosis in recent years in Brazil. (A) Cases of human sporotrichosis have been reported in 25 of 26 Brazilian states, with significant differences in their frequency. **(B)** The South and Southeast states of Brazil show the largest epizootic feline sporotrichosis in the world. Currently, the zoonotic sporotrichosis driven by S. brasiliensis is expanding rapidly in Northeast Brazil. Image from Rodrigues *et al.*, 2020.

1.3. Sporotrichosis treatment and control strategies

Prevention and control strategies with the engagement of animal and human health policies are essential to reduce public health risks due to this zoonotic outbreak, especially in high-density populated urban areas where cat transmission is predominant (24). The neutering of the cats is an important preventive and control policy, since it diminishes the instinct for hunting, mating, and roaming, thus reducing the chance of transmission of Sporothrix spp. (36). Cytopathological examination or other rapid preliminary diagnostic tests with good sensibility can also be helpful since early feline sporotrichosis treatment contributes to disease control in the community (37).

Although human sporotrichosis is generally responsive to standardized antifungal strategies (2), feline sporotrichosis treatment is a challenge for both veterinarians and the infected cat owners, demanding a long period of daily care, cooperation, and persistence (1). Sporotrichosis therapy strategy and prognosis depend on the feline medical condition, the etiological agent, disease severity and its clinical signs, such as number, extension, and lesion location (1). Independently of the treatment regimen, a crucial therapeutic approach is to persevere with it for at least 1 month after the complete resolution of the cutaneous lesions, which may take from a few weeks to several months (median time, 4–9 months), to assure clinical cure (8,29,36). Felines undergoing systemic antifungal therapy do not appear to play a key role in the Sporothrix spp. transmission cycle (37) and clinical cure is observed regardless of co-infection with feline immunodeficiency virus and/or feline leukaemia virus (36).

Treatment abandonment can be frequent, either in the first month (30) or from the second to sixth month of therapy, upon clinical improvement (38). The long-during struggle to keep infected cats isolated and confined, administrate oral medications, and transport them to the clinic together with the treatment cost have been described as major treatment abandonment causes. Additionally, since factors such as non-visualization of skin lesions and systemic involvement may lead to misperception of cure, there is a risk of disease recurrence if treatment is discontinued before the therapeutic protocol established by the veterinarian (38).

There are few prospective studies available regarding sporotrichosis treatment in animals. For that reason, evidence-based treatment options come from retrospective studies and case reports (39). The antifungal treatments available for feline sporotrichosis are azole derivatives, such as itraconazole and ketoconazole, triazole derivatives, such as fluconazole and posaconazole, sodium and potassium iodides, amphotericin B and terbinafine (40). Although sporotrichosis etiological agents have a susceptible response profile to antifungal drugs, several reports of drug resistance have already been recently reported (6,7).

Despite not inducing an active immune memory response by the host, antibody treatment is another way to combat pathogens aiding to neutralize infection. A specific and protective humoral response against *Sporothrix* spp. cell wall has already been observed (41,42). A major antigen candidate is a 70-kDa glycoprotein (gp70), whose antibodies showed promising results against *S. globosa* (43) and *S. brasiliensis* (44). Despite all efforts, until this day there is no immunoprophylaxis or immunotherapy available to humans or cats against Sporothrix spp (36).

1.4. Components and virulence factors

Pathogen microorganisms need to express virulence factors to become virulent, but changes in the host which alter the host-microbe interaction can often be determinant for the disease to occur (45). Consequently, there is a great interest in microbial pathogenesis research, with the ultimate goal to develop therapies that target these virulence factors. However, the virulence traits involved in the establishment, development, and severity of sporotrichosis are still not well understood (46).

In two experimental studies using murine models, Arrillaga-Moncrieff and co-workers (4,47) observed significant differences between mice infected with *S. schenckii* and *S. brasiliensis*, whereas the latter showed more virulence, presenting higher mortality, greater dissemination capacity and massive infiltration in infected tissues. After these findings, although different inoculation methods were used, other authors found similar results with the same type of model, endorsing that several *S. brasiliensis* strains have increased pathogenicity when compared to *S. schenckii* and other species (18,48,49).

Della Terra (50) studies in mice models elucidated that not only *S. brasiliensis* virulence is strain-dependent, but also that feline isolates were more virulent than those of human origin, while in Castro's experiment (48), skin lesions caused by subcutaneous inoculation of *S. brasiliensis* strains in mice were usually more progressive, persistent, and wider than lesions caused by *S. schenckii*.

Additionally, a higher degree of pathogenicity in felines (20) and humans have also been reported (51) and correlated to severe and atypical clinical manifestations (49). Among all species pathogenic to mammals, the most virulent and with the most impactful clinical manifestations is *S. brasiliensis* (4,49,50). Contrastingly, *S. schenckii* exhibits a varying range of virulence while *S. globosa* seems to be the less virulent species from the pathogenic clade of Sporothrix species (6).

Despite the role of dimorphism, thermo-tolerance, and melanin, *Sporothrix* virulence factors are still not clearly understood (21,52,53). *S. brasiliensis* and *S. schenckii* are highly syntenic, sharing a 97.5% average sequence identity and a similar genome size of, respectively, 33.2 Mb and 32.4 Mb

(54,55). Since an *in-silico* analysis of both genomes does not appear to explain *S. brasiliensis* higher virulence (55), a narrower clarification of the mechanisms underlying *S. brasiliensis* virulence is required.

Fungi from the *S. schenckii* complex exhibit a thermal dimorphic behaviour, which has been described as a virulence factor in several other fungi that are pathogenic to humans, such as *Candida albicans*, *Histoplasma capsulatum* and *Paracoccidioides brasiliensis* (17,56–59). The morphological shift toward environmental alterations may represent an important feature for animal infection and virulence (5,17), but the mechanisms regulating thermal dimorphism are not fully understood. However, temperature, pH, oxygen, nutrient availability, and calcium uptake affect this trait (17).

Melanins are polymeric aromatic dark pigments, produced from a wide variety of organisms, from bacteria and fungi to mammals. In addition to the common and vital effect in protecting against radiation, more specific roles have been found in different species (60). Melanin-producing pathogenic fungi are more resistant to both harsh environmental circumstances and conditions imposed by host immune defense (61). Melanisation confers *in vitro* resistance to a wide range of challenges commonly found in fungal habitats, such as extreme temperatures, acidity, oxidative conditions and exposure to radiation or heavy metals (62). In pathogenic fungi, melanin pigments also inhibit phagocytosis and fungicidal activity by mammalian host cells, thus protecting the fungi against the host's innate immune response (63). Additionally, melanin pigments also confer protective effects against antifungal drugs in several fungi species, which includes members of the *Sporothix* genus (61). *Sporothrix* melanin is important for sporotrichosis deep organ dissemination since it can impair host innate and adaptive immunity, by inhibiting phagocytosis, fungicidal activity of reactive oxygen species, macrophages digestive functions and antigen presentation (64).

1.5. Immune response in *Sporothrix* infection

The immune system is a collection of cells, chemicals and processes whose combined functions protect the host from foreign antigens, such as viruses, microbes (organisms such as parasites, bacteria, and fungi), toxins and cancer cells (65). Innate and adaptive immunity are the two fundamental lines of defense of the immune system against pathogens when structural and chemical barriers were not capable to block intruding pathogens (65). Innate immunity, as the first immunological mechanism for fighting against an intruder, is a rapid response that has no antigen-specific immunologic memory (65), only long-term metabolic rewiring features (66). Adaptive immunity is an antigen-specific immunological mechanism, which has the capacity for immunological memory. Although at the first encounter adaptive

immunity portraits as a slow defense mechanism, it enables the host to promote a more rapid and efficient immune response upon subsequent exposure to the same antigens (65).

Innate and adaptive immune systems synergize together to promote the immune response towards pathogens, in a way that defects in either system can provoke illness or disease, such as hypersensitivity reactions and inappropriate inflammation, autoimmune diseases and immunodeficiency disorders (65). Pathogen microorganisms need to express virulence factors to become virulent, but changes in the host which alter the host-microbe interaction can often be determinant for the disease to occur (45). Immunosuppressed patients, by immunosuppressive therapy or HIV infection, often develop sporotrichosis disseminated forms (6,31,51,67).

The exact role of immune cells in *Sporothrix* spp. infection is not yet fully elucidated, but macrophages are probably the most important immune cells for containing and terminating sporotrichosis (68,69) since their phagocytic activity plays a crucial role in surveillance and clearance of fungal pathogens (70,71). Macrophages can recognize, through pattern recognition receptors (PRRs), some pathogen associated molecular patterns (PAMPs) of *Sporothrix*. These PAMPs are constituents of fungus cellular surface, which allows adherence, engulfment, respiratory burst, and secretion of pro-inflammatory or anti-inflammatory biological mediators to control the infection (68,69). However, several factors can interfere with the efficiency by which phagocytes recognize, internalize, and kill fungal pathogens, such as shape, size, cell wall composition and fungal intrinsic immune evasion mechanisms (64,69,72).

TLR-2 and TLR-4, along with Dectin-1 and Mannose receptors are PRRs that promote fungal recognition and macrophage inflammatory activation to Sporothrix spp (69). These receptors activate the innate immune response by recognizing specific pathogen-associated molecular patterns (PAMPs) on pathogen cell surfaces (68). Macrophage toll-like receptors (TLR) have been directly associated with PAMP recognition and immune response triggering from several fungi, such as *Aspergillus fumigatus, Candida albicans, Cryptococcus neoformans, Pneumocystis jirovecii, S. schenckii*, and *S. brasiliensis* (68,73–78). Moreover, TLRs belong to a family of recognition receptors that link the innate and acquired immune system (79), and TLR2 and TLR4 are specifically important to the innate immune response against *S. brasiliensis* and *S. schenckii* (68,75).

In fungal infections, the first contact between the host and the pathogen is through the interaction between the immune cells and the fungal cell wall (CW). Its composition plays a crucial role in pathogenesis and immunogenicity by inducing a cellular and humoral immune response (69), and the three main components are ß-glucans, chitin, and mannans (80). Soluble and lipidic antigens of the fungal CW surface can activate macrophages via TLRs (68,75). This activation together with the humoral

immunity mediated by specific antibodies to components of *Sporothrix* spp, play a leading role in the infection progress (42,81).

Several components and exoantigens in the fungal CW are potentially involved in immune evasion and higher virulence in *S. brasiliensis*, such as the presence of a 70-kDa glycoprotein, certain lipids, peptido-rhamnomannan, and the polysaccharide composition (46,82–85). Exoantigens present in the CW of the *Sporothrix* spp., such as the peptido-rhamnomannan, are efficient inhibitors of the production of cytokines such as IL-1β, IL-6, TNF, IL-12, and IL-10 (68,75,84). Additionally, *Sporothrix* spp. thermal dimorphism alters its CW components, which can modulate macrophages' inflammatory response. The interaction with the CW of conidia induces a lesser pro-inflammatory response and a lower rate of ROS-induced cell death when compared to yeast (86).

1.6. Agrobacterium tumefaciens-mediated transformation (ATMT)

The incorporation of exogenous DNA into a cell is called transformation, an important tool to link genes to functions and consequently better understand one microorganism pathophysiology (87). Protoplast-mediated transformation (PMT) is the most common method to incorporate exogenous DNA in fungi. The creation of a fungi protoplast and PMT first requires the removal of its cell wall. Since the cell wall composition varies between fungi species, this technique becomes a laborious technique that requires standardization for the cell wall removal to each fungal species used (88). The *Agrobacterium tumefaciens*-mediated transformation (ATMT) technique removes this process altogether, since the desired gene sequence can be inserted not only into protoplasts but also into intact cells (89), thus avoiding the laborious protoplasts preparation process.

Agrobacterium tumefaciens is a Gram-negative soil phytopathogen that was discovered almost 100 years ago as the causative agent of crown gall disease (90) among most of the plant families inside the plant kingdom (91). Through a type IV secretion system, this bacterium is capable to induce tumours by transferring part of its DNA (T-DNA), located on a tumour-inducing (Ti) plasmid, to the host (92). Naturally, the T-DNA inside the Ti plasmid encode enzymes that influence the production of plant growth regulators, resulting in the crown gall disease (Michielse et al., 2008). However, the manipulation of its Ti plasmid made this species a central genetic tool in diverse fields of biological and biotechnological research (93).

ATMT was first applied as a genetic engineering technique which offers an efficient tool for random insertional mutagenesis in plants' genomes. However, under laboratory conditions, it was found that the *Agrobacterium* range of eukaryotic organisms that could be genetically transformed is much

broader (94). The ATMT technique has already transformed yeast (95), filamentous fungi, cultivated mushrooms (96), cultured human cells (97), and even *Sporothrix* schenckii (98–100).

In the plant kingdom, the T-DNA is integrated by illegitimate recombination, being randomly inserted into the genome (101). Contrastingly, in yeast and fungi, the T-DNA is often inserted through homologous recombination. This difference allows the possibility of targeted integration of the foreign DNA, if its shares sequence homology with the host genome, thus providing genomic tools for insertional mutagenesis or specific gene replacement (94). Furthermore, the non-sequence-specific manner that *Agrobacterium* integrates its T-DNA within the host genome is vital to produce many mutants when transforming intact cells, such as conidia, mycelium, and yeasts (98).

The ATMT has already been standardized in thermodimorphic fungi (102–108) and *Sporothrix schenckii* (98–100), but the use of this technique in *S. brasiliensis* is scarce (109). ATMT technique has proven to be a useful genetic tool to unveil several pathogen pathophysiology mechanisms (50,99). An attempt to standardize this technique on *S. brasiliensis* is important to construct large-scale transformant libraries, which can help to open new insights into exploring more effective disease control strategies for sporotrichosis, by better understanding its host-pathogen interactions and virulence mechanism.

CHAPTER 2

Aims and Outline

The mechanism involved in *Sporothrix brasiliensis* increased virulence and aggressiveness are yet to be clarified. Targeted fungal transformation is an important tool which permits the identification of molecular mechanisms and cellular processes involved directly in the virulence of the target microorganism, and thus, can clarify the role of gene functions *in vitro* and *in vivo*. The first step to achieve this goal is the development of an easy, quick, and reproducible methodology for transformation of *S. brasiliensis.* Secondly, the design and creation of strains with fluorescent proteins is an important technology which could facilitate the execution of *in vitro* and *in vivo* infection assays with *S. brasiliensis*. Therefore, our main objectives were to:

1. Establish a protocol and optimizations for an efficient *Agrobacterium tumefaciens*-mediated transformation (ATMT) of *S. brasiliensis*.
2. Design, create and categorize *S. brasiliensis* strains with fluorescent proteins.
3. Perform human monocyte-derived macrophages (MDMs) infections with fluorescent strains *S. brasiliensis* and evaluate its applicability.

The work presented in this thesis aims to contribute for the development of molecular tools to unravel the virulence mechanisms of *S. brasiliensis*, as well as to create fluorescent strains and evaluate their applicability in *in vitro* models of infection.

Chapter 1 presents an introduction to the state of art of sporotrichosis, its etiologic agents, the immune response to *Sporothrix* spp. and the ATMT technique. Firstly, a brief description of the disease is presented, its clinical forms, epidemiology, diagnosis, and treatment. Secondly, the virulence factors and the immune response to Sporothrix spp. are also described. Lastly, the state of art of the ATMT technique is introduced.

Chapter 2 describes the aims of this dissertation and its outline.

Chapter 3 focus on the establishment of an ATMT protocol to produce *S. brasiliensis* transformants. The effects of several parameters were evaluated on the transformation efficiency, such as, time, ratio bacteria:fungi, sterile membranes and strains used in the co-cultivation. To summarize, from the analysis of the tested conditions, we concluded that 26°C for 72h, using a 2:1 ratio (bacteria:fungi), using the *A. tumefaciens* AGL-1 and *S. brasiliensis* ATCC 4823 are the best conditions for ATMT of *S. brasiliensis*. Overall, we were able to develop a protocol for transformation of *S. brasiliensis* using ATMT with high transformation rates and mitotic stability.

In *Chapter 4, S. brasiliensis* pGAPDH::GFP and pGAPDH::H2A::GFP strains with fluorescent proteins in the cytoplasm and the nucleus, respectively, were used assay to assess several antifungal mechanisms. The pGAPDH::GFP strains still had a detectable amount of GFP fluorescence upon

phagocytosis and thus, can be used without fluorophore stain prior to infection. On the other hand, the loss of GFP fluorescence by the pGAPDH::H2A::GFP strain inside the macrophages preclude there use in downstream assays since we were unable to correlate the loss of GFP fluorescence of the pGAPDH::H2A::GFP strain with the loss of viability and/or death after monocytes/macrophages engulfment in both microscopic and FACS analysis.

Chapter 5 presents a broad discussion and future perspectives regarding this thesis.

CHAPTER 3

Optimization of *Agrobacterium tumefaciens*-mediated transformation on *Sporothrix brasiliensis*

Abstract

Sporothrix brasiliensis is the most virulent etiological agent that causes sporotrichosis, the most prevalent mycosis worldwide and a hyperendemic in Brazil. The virulence factors which result in the *S. brasiliensis* worst phenotype, when compared to the rest of the Sporothrix pathogenic clade, remain poorly understood. The development of genetic engineering techniques for *S. brasiliensis* transformation is urgently needed to better understand the association of specific genes and functions, unravelling this microorganism pathophysiology. In this work, we optimized the protocol for its genetic manipulation using the *Agrobacterium tumefaciens*-mediated transformation (ATMT) system. Several conditions already pre-established in other fungi were tested its effect on the ATMT efficiency. Our results point to 72h of co-cultivation, the AGL-1 strain and the 2:1 ratio (bacteria:fungi) as ideal conditions for a high number of transformants. In these conditions, we obtained 3179 ± 1171 transformants/co-cultivation. No statistical differences were found between the Hybond™-C e Hybond™-N+ sterile membranes used. Additionally, the ATCC 4823 and 4858 *S. brasiliensis* strains produce more transformants. Only the co-cultivation temperature of 26°C was used. The ATMT methodology used is an efficient tool for mutagenesis in *S. brasiliensis*.

3.1. Introduction

Sporotrichosis is the world's most prevalent and distributed subcutaneous mycosis. This disease etiological agents belong to the *Sporothrix* pathogenic clade (1,3), characterized by several thermodimorphic fungi from the genus *Sporothrix* growing as yeast in infects mammals (16). Among all species pathogenic to mammals, the most virulent and with the most impactful clinical manifestations is *S. brasiliensis* (18,48–51). However, there is yet a limited genetic manipulation tool repertoire for the *Sporothrix* genus (110), and despite the role of dimorphism, thermo-tolerance, and melanin, *Sporothrix* virulence factors are still not clearly understood (54).

Agrobacterium tumefaciens-mediated transformation (ATMT) offers an efficient tool for random insertional mutagenesis. This bacterium can transform intact cells, such as conidia, mycelium and yeasts while still producing many mutants due to its non-sequence-specific manner of T-DNA integration within the host genome (98). Although ATMT has already been standardized for *S. schenckii* (98–100), the information about the use of this technique in *S. brasiliensis* is scarce. ATMT technique has proven to be a useful genetic tool to unveil several pathogen pathophysiology mechanisms (50,99), thus an attempt to standardize this technique on *Sporothrix brasiliensis* is justifiable.

Here, we report the establishment of an ATMT system of *S. brasiliensis*, with an analysis into the important factors affecting the transformation efficiency. We report an efficient, simple, and reproducible transformation method which enabled us to obtain many T-DNA insertional mutants within a two-week experimental period.

3.2. Materials and Methods

3.2.1. Microorganisms and culture conditions

The *S. brasiliensis* ATCC MYA-4823, ATCC MYA-4824, and HUPE 114158 were used for fungal transformation. Their origin is better described in Table 1. The ATCC MYA-4823 strain was cultured at 37°C for 72h in yeast extract peptone dextrose (YPD) medium (2% glucose, 2% peptone, 1% yeast extract; for solid medium 1.5% agar was added; pH = 7.8), while both the ATCC MYA-4824 and HUPE 114158 strains were cultured in Brain Heart Infusion Broth (BHI) medium (3.7% Biolife™ BHI; for solid medium 1.5% agar was added; pH = 7.8). All cultures were maintained at 4°C for short-term storage and were routinely sub-cultured every 4–6 weeks. Yeasts were obtained through sterile gaze filtration.

Table 1. *S. brasiliensis* strains used in this work.

Isolate	Another name	Isolation	Source	Citation	Virulence	Origin
ATCC MYA-4823	5110	Brazil	Feline skin lesion	(48,54,109,111)	High (48)	Bought at ATCC®
ATCC MYA-4824	IPEC 17943	Brazil	Feline skin lesion	(48,112)	Low (48)	Kindly donated by Lopes-Bezerra, L. M.
HUPE 114158	Ss58	Brazil	Human cutaneous with facial destruction	(48,109)	High (48)	Kindly donated by Lopes-Bezerra, L. M.

The *A. tumefaciens* strains AGL-1 (113,114), EHA105 (114), and LBA1100 (103,109), harboring the commercially available pUR5750 plasmid (Figure 6A) (96), were used to perform ATMT and evaluate its efficiency, due to this plasmid hygromycin B phosphotransferase (HPH) gene. All *A. tumefaciens* cells were cultured at 26°C in solid LC Broth medium supplemented with the antibiotics rifampicin (20μg/ml) and kanamycin (100μg/ml) and maintained at 4°C for short-term storage. The *A. tumefaciens* strains used were kanamycin-resistant and harboured two distinct plasmids, as schematized in Figure 6B. The first plasmid was the Ti plasmid, which carries the spectinomycin resistance gene along with virulence promoting genes. The phenolic compound acetosyringone (AS) induces the expression of the Vir domain inside the Ti plasmid, which leads to the generation, transference, and random integration of the T-DNA, present in the constructed plasmid, into the recipient cell's genome (88,92,115). The binary vector used

was the plasmid pUR5750 (Figure 6B). It had the gene of resistance to kanamycin in *A. tumefaciens* and *Escherichia coli*, and the T-DNA constructed to insert a specific gene inside the host genome, in this case, the HPH gene.

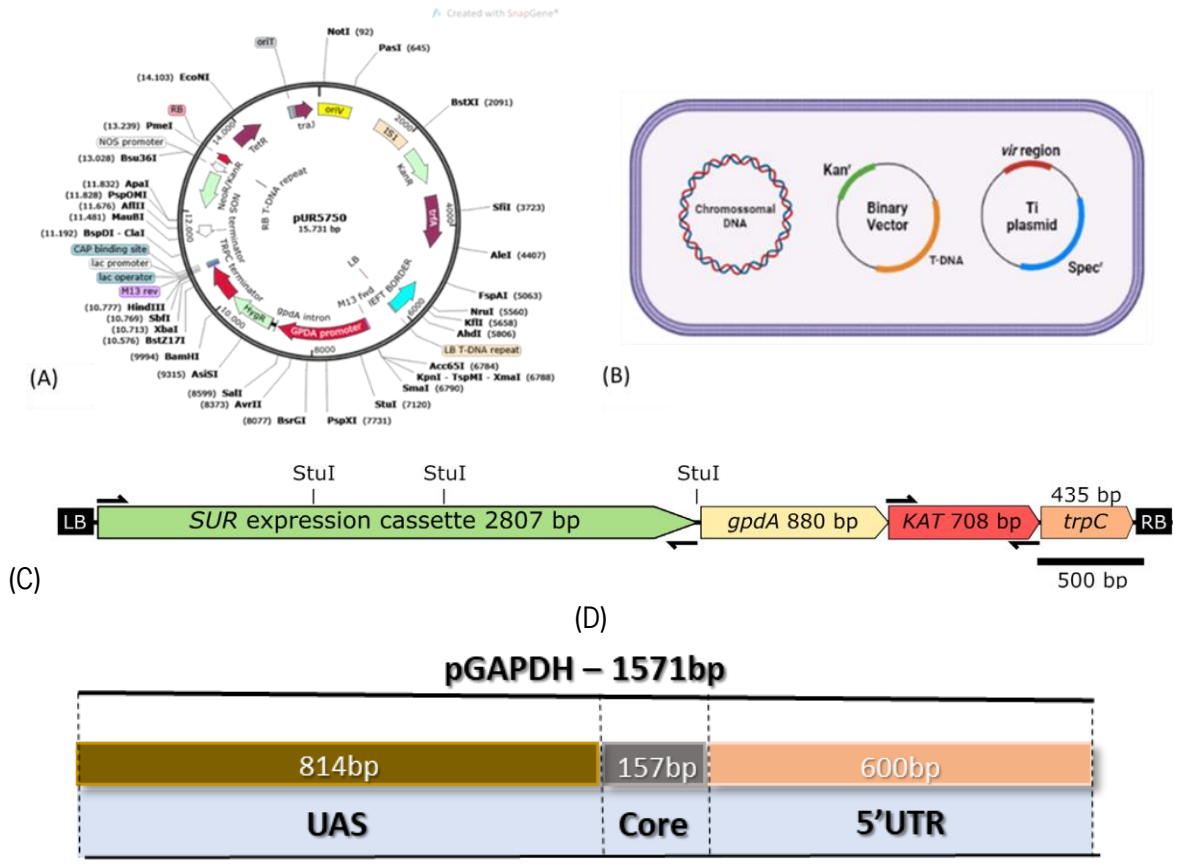

Figure 6. Schematic representation of the system used for A. tumefaciens-mediated transformation. (A) The A. tumefaciens carried two distinct plasmids and chromosomal DNA. Image adapted from Michielse et al., 2008. **(B)** The binary vector used was the plasmid pUR5750. **(C)** Schematic representation of the pPZP201BK::SUR::gpdA::Kat::TrpC plasmid. Image from Sbaraini et al., 2021. **(D)** Schematic representation of the pGAPDH::GFP plasmid.

The second plasmid used, pPZP201BK::SUR::gpdA::Kat::TrpC (Figure 6C), was designed by Sbaraini (116) to produce transformants that express and accumulate the far-red fluorescent protein TURBOFP635/Katushka in the cytoplasm. This plasmid uses the selection marker Magnaporthe grisea acetolactate synthase enconding gene (SUR gene), which confers resistance to Chlorimuron ethyl (116,117). Using two selection markers allow the production of mutants with two fluorescent proteins upon consecutive ATMTs. The last plasmid used in the ATMT was the pPST608::pGAPDH::GFP (Figure 6D), to produce strains that express and accumulate the GFP in the cytoplasm, for the mitotic stability analysis.

3.2.2. Inoculum count optimization for future experiments *in vitro*

Several protocols performed in this thesis required a quick and accurate way to obtain *S. brasiliensis* inoculums for experiments *in vitro*. To optimize the inoculum concentration, exponential growth cells were acquired through culture at 37°C for 24h in liquid YPD (pH 7.8) medium and sterile gaze filtration. Samples had their optic density (OD_{660nm}) adjusted to several values ranging from 0.1 up to 1 and the number of cells was counted by both the Neubauer chamber counting technique and by counting the number of Colony Forming Unit (CFU) after 7 days of culture at 37°C in a YPD (pH 7.8) solid plates. Linear regression was performed to obtain the linear correlations between the concentration of exponential growth *S. brasiliensis* ATCC 4823 yeast cells, the Neubauer chamber count and the optic density (OD_{660nm}).

3.2.3. *Sporothrix brasiliensis* sensitivity analysis to Hygromycin B and Chlorimuron ethyl

Transformation systems can take advantage of the resistance markers, such as the HPH and SUR resistance genes (117,118), which confer resistance to Hygromycin B (HygB) and Chlorimuron ethyl (CE), respectively. To create mutants with these resistance markers, the minimum inhibitory concentrations of these antibiotics for *S. brasiliensis* ATCC 4823 were first evaluated. To analyze cell growth in selective YPD (pH 7.8) solid and liquid medium (100), exponential growth *S. brasiliensis* ATCC 4823 wild-type cells were acquired through culture at 37°C for 24h in liquid non-selective YPD (pH 7.8) medium and sterile gaze filtration.

To analyze the resistance to Hygromycin B and Chlorimuron ethyl, cell growth was evaluated respectively in both liquid and solid medium of the selective YPD (pH 7.8) and Yeast Nitrogen Base (YNB) liquid medium (0.16% BD Difco™ YNB, 2% glucose, 0.5% ammonium sulfate, 25 µg/mL of leucine, 25 µg/mL of histidine, 25 µg/mL of methionine and 25 µg/mL of uracil) (100,116,117). Exponential growth S. brasiliensis ATCC 4823 wildtype cells were acquired through culture at 37°C for 24h in liquid non-selective YPD (pH 7.8) medium and sterile gaze filtration. Cell density was adjusted to an OD660nm of 0.1 by the Genesys™ 20 Spectrophotometer (Sigma-Aldrich, model Z376035) in both mediums. Fungal growth was evaluated by measuring absorbance at 660nm after incubation at 37°C for 24 hours with reciprocal shaking at 200rpm in several antibiotic concentrations.

To define the minimum inhibitory concentration of HygB (Formedium™, Hunstanton, England) and CE (Santa Cruz Biotechnology, Dallas, USA) in *S. brasiliensis* in solid YPD and YNB mediums, cells were diluted to three concentrations: 10^8, 10^7, and 10^6. Those concentrations were then inoculated into

mini plates containing solid medium YPD (pH 7.8), with different concentrations (µg/mL) of each antibiotic. HygB plates had the concentrations of no antifungal present, 25, 50, 75, 100,150, 200, and 250µg/mL. The CE plates had concentrations of no antifungal present, 5, 10, 15, 20, 25, and 30µg/mL. For each mini plate, 5µL of each dilution was inoculated: 10^8 on the left border, 10^7 on the middle, and 10^6 on the right border. All the mini plates were put at 37°C for seven days, and a visual (qualitative) comparison was made at the end.

3.2.4. *Agrobacterium tumefaciens*-mediated transformation protocol of *Sporothrix brasiliensis*

The transformation procedure was based on previously described protocols (92,98,99,109), with some modifications, and schematized in Figures 7 and 8.

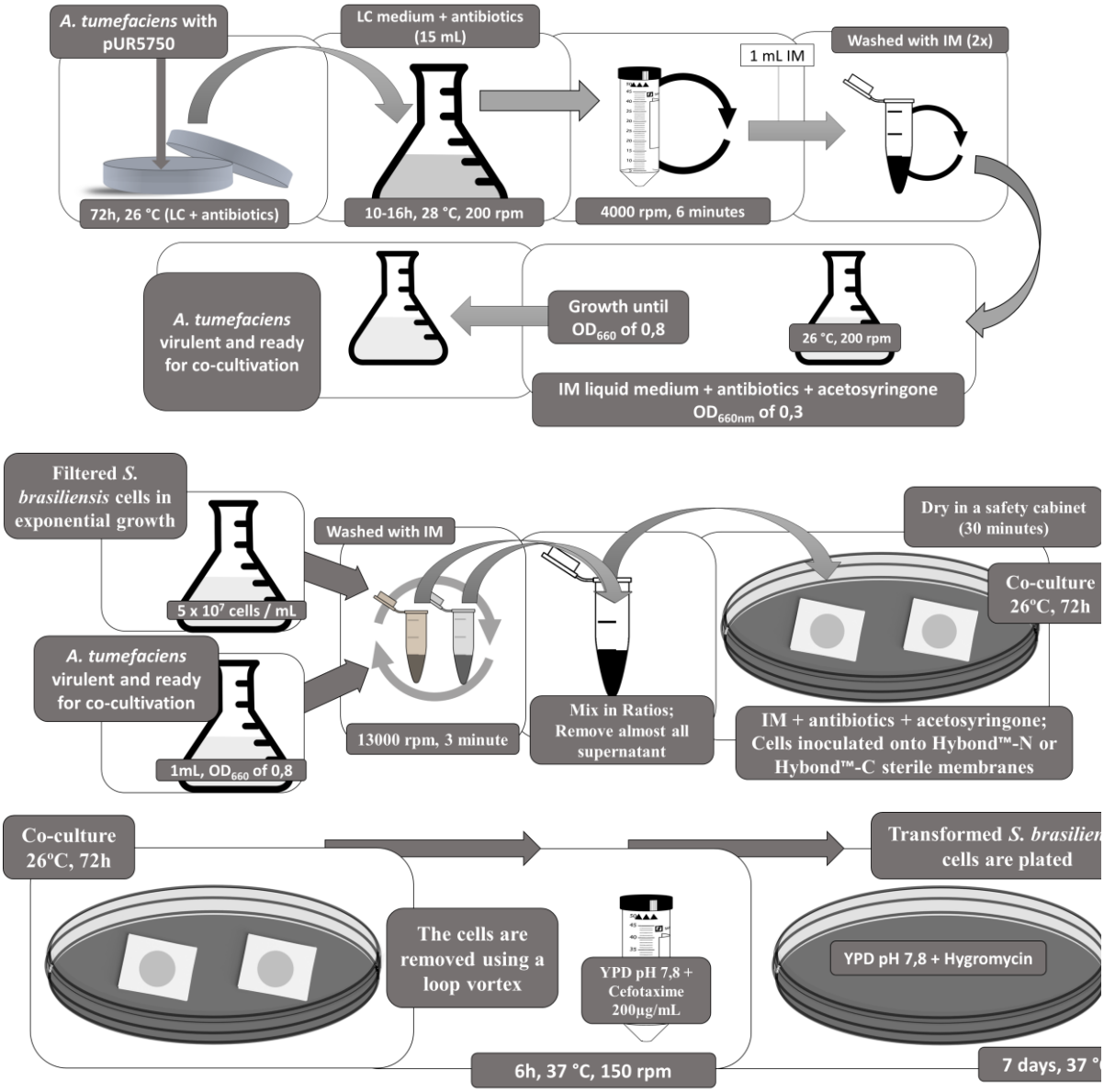

Figure 7. Schematic of *S. brasiliensis* ATMT technique.

Each *A. tumefaciens* strain cells were cultured at 28°C while shaking (200 rpm) in 10 mL LC broth supplemented with antibiotics for 6-10h. Subsequently, the culture was centrifuged at 4000 rpm for 6 min and the pelleted cells were resuspended with Induction Medium (IM) (92) with 200μM of acetosyringone (AS), to an optic density (OD_{660nm}) of 0.3. The culture grew overnight at 26°C with shaking to an OD_{660nm} of 0.6–0.8, to acquire virulence. In parallel, exponential growth fungal cells were cultured at 37°C for 24h while shaking (200 rpm) in 50mL YPD (pH 7.8), or BHI in the case of the ATCC 4858 strain, and yeast cells were obtained through sterile gaze filtration.

Each *A. tumefaciens* strain was mixed with *S. brasiliensis* cells, at two different ratios. Inside the 1:1 ratio, 5 x 10^7 cells of each species were used, while the 2:1 ratio had double the amount of *A. tumefaciens* cells (1 x 10^8). Those mixtures were centrifuge and had their supernatant removed to an approximate final volume of 100μL, and were inoculated on a sterile membrane, onto solid IM plates. Four co-cultivation periods in the dark (24h, 48h, 72h, and 96h) and two different sterile membranes were compared (Hybond™-C and Hybond™-N+, 0.45μm pore, GE Healthcare Limited, Amersham, UK). Before incubation, the plates were air-dried in a safety cabinet with the lights off for approximately 30 minutes (103).

Next, after each period of co-cultivation, the membranes were transferred to falcon tubes and the cells dislodged into a 5mL YPD medium (pH 7.8) containing cefotaxime (200μg/mL, Formedium™, Hunstanton, England), for growth inhibition of *A. tumefaciens*. Lastly, after 6h of cultivation at 37°C, while shaking at 200 rpm, 1mL were centrifuged, 800μL of supernatant was removed and the final volume of 200μL was inoculated on a selective YPD solid medium (hygromycin B, 150 μg/mL, Formedium™, Hunstanton, England). Since the ATCC 4824 and 4858 strains did not grow properly in YPD, their cells had to be instead respectively inoculated in the selective BHI medium (with hygromycin B, 150 μg/mL, Formedium™, Hunstanton, England). Only to produce transformants with the plasmid pPZP201BK::SUR::gpdA::Kat::TrpC, the final volume of 200μL was inoculated on a selective Yeast Nitrogen Base (YNB) solid medium (0.16% BD Difco™ YNB, 2% glucose, 0.5% ammonium sulphate, 25 μg/mL of leucine, 25 μg/mL of histidine, 25 μg/mL of methionine and 25 μg/mL of uracil), with Chlorimuron ethyl (30μg/mL, Santa Cruz Biotechnology ™, Dallas, USA) instead of hygromycin. Fungal cells without the transforming agent *A. tumefaciens* were inoculated into selective and non-selective YPD mediums, as a positive and negative control, respectively. Lastly, after cultivation for a week at 37°C, the number of transformants was counted, scaled to the total amount of selective medium used (5mL), and compared between each condition. To compare different conditions for the ATMT protocol, only the *S. brasiliensis* ATCC 4823 was used.

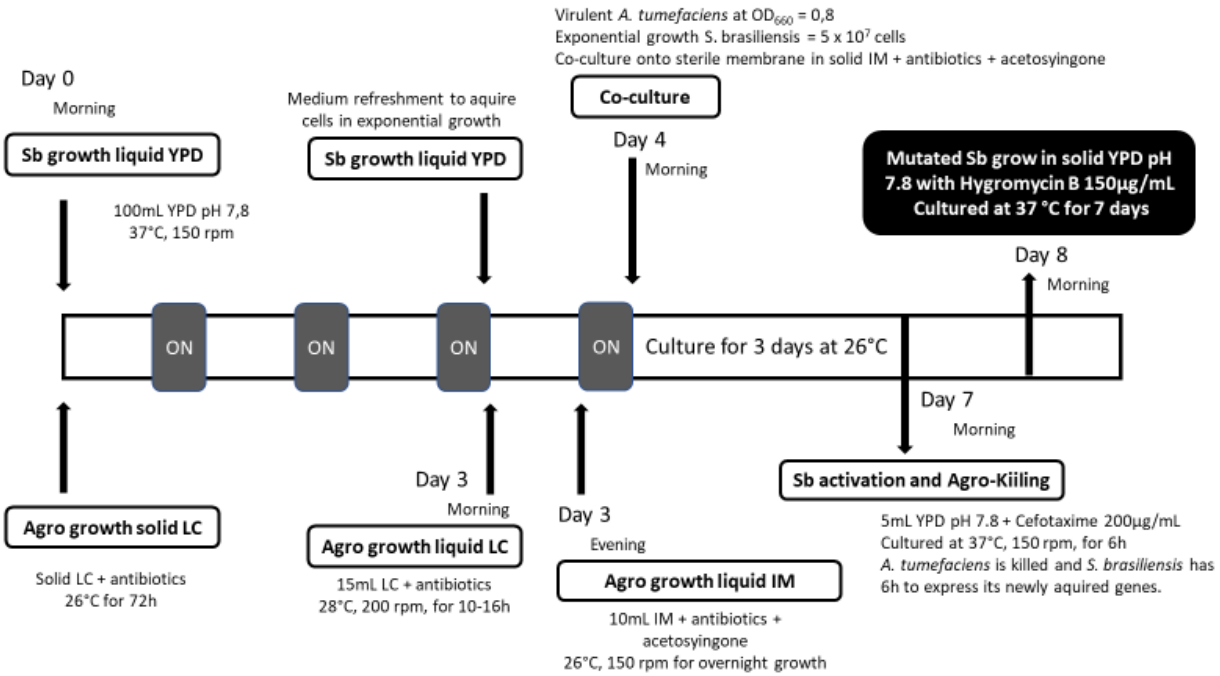

Figure 8. Timeline schematic of *S. brasiliensis* ATMT.

3.2.5. Characterization of isolated transformants

To investigate and confirm the integration of T-DNA of the HygB^R isolates, the HPH gene copy number in five *S. brasiliensis* was determined by the standard curve method (Cts plotted against the logarithm of the DNA copy number) (119). To that, five transformants had their DNA extracted.

For DNA Extraction, each *S. brasiliensis* transformant and the wild-type isolate were grown for 72h in YPD pH 7.8 and then transferred to falcons, where the YPD medium was exchanged for sterile distilled water. A volume of 300µL from each culture was centrifuged, had its supernatant removed, was moved to microtubes, and then resuspended in 350µL of lysis buffer [1mM EDTA, 10mM Tris–HCl (pH 8.0), 1% SDS, 100mM NaCl, 10mg/mL RNAse A (GRiSP, Porto, Portugal)]. After glass beads addition, 80µL of TE buffer (X1, pH 7.6) and 150µL of phenol:chloroform:isoamyl alcohol (25:24:1; pH 8.0) were added. Cell mechanical disruption was performed by vortexing for 1 minute. After centrifugation (14,000 rpm, 5 min), the aqueous supernatant was carefully collected and moved to another microtube. A volume corresponding to 10% from the aqueous supernatant removed was added of sodium acetate (3 M) and 250% of absolute ethanol to each microtube. After incubation at 0°C for 15 minutes on ice and centrifugation (14,000 rpm, 4°C, 10 min), the supernatant was removed, and 400µL of ethanol 70% (vol/vol) was added to remove salts and small organic molecules. The solution was centrifuged again (14,000 rpm, 0°C, 5 min), its supernatant was removed, and the pellet was air-dried inside the Bunsen burner range. Lastly, the pellet was resuspended in 50µL of TE buffer (X1, pH 7.6). TE buffer (1x) was

used as blank, and the samples were stored at -20°C. The extracted DNA was assessed using ND-100 UV-Visible light spectrophotometer (Nanodrop Technologies, Wilmington, United Kingdom).

Lastly, the single copy references of the Actin-β gene and the glyceraldehyde-3-phosphate dehydrogenase (GAPDH) gene were quantified in parallel with HPH in transformants and wild-type genomic DNA. Two wild-type isolates were used as control. Primers used for the copy number analysis are listed in Table 2.

Table 2. Primers list from copy number analysis.

RT_LP_actin beta	GATCGGTATGGGCCAGAAGG
RT_RP_actin beta	GGATACCACGCTTCGACTGT
RT_LP_GAPDH	TGCCTCCTACGACGAGATCA
RT_RP_GAPDH	GTGTAGCCGAGAATGCCCTT
RT_LP_HPH	GATGTAGGAGGGCGTGGATA
RT_RP_HPH	ATAGGTCAGGCTCTCGCTGA

Isolates from the ATMT with plasmid pPZP201BK::SUR::gpdA::Kat::TrpC were characterized by microscopic evaluation of the presence of the far-red Kat-fluorescence protein, TURBOFP635/Katushka. Transformants and wild-type cells were obtained during exponential growth. To obtain yeast cells and mycelium at exponential growth, cells were cultivated in a selective YNB medium at 37 and 26°C, respectively. Fluorescence microscopy analyses were performed with the Olympus Widefield Upright Microscope BX61 by either bright-field (upper panel) or fluorescent microscopy (lower panels). All images were captured using 395nm/509nm for excitation and emission, respectively, and exposition time to the laser beam was automatically set.

3.2.6. Mitotic stability

After molecular characterization of the *S. brasiliensis* transformants, their mitotic stability was determined by analysing the stability of the Green fluorescent protein (GFP) gene, present in the genome of the pGAPDH::GFP transformants (Figure 18). To achieve that, five randomly selected transformants and wild-type strains were successively cultured without hygromycin B for five generations on a YPD medium (pH 7.8) at 37°C for 12h, while shaking at 200rpm. For each restreak, cells were fixed with 500µL of 2% paraformaldehyde for 15 minutes at room temperature and thirty thousand events were captured using Fluorescence-activated cell sorting (FACS). The wild-type MFI was used to determine the MFI autofluorescence threshold, and consequently the percentage of population cells that did not express GFP throughout five generations.

3.2.7. Statistical analysis

Data are reported as the mean ± standard error of the mean (SEM) of at least two independent assays with two or three replicates each. The statistical analysis was performed using GraphPad Prism Software version 8.0 (GraphPad Software Inc, California, USA, https://www.graphpad.com/scientific-software/prism/). The normality assumptions were assessed in all cases using the Shapiro-Wilk test. A student's t-test was used to analyze the differences in the average number of HygBR clones for co-cultivation temperature and the use of sterile membranes. Differences regarding the time, ratio of co-cultivation, and strains used were analyzed using One-Way ANOVA. Statistically significant values are indicated as follows: *p ≤ 0.05, **p ≤ 0.01, ***p ≤ 0.001 and ****p ≤ 0.0001.

3.3. Results

3.3.1. Inoculum count optimization for future experiments in vitro

Several protocols performed in this thesis required a quick and accurate way to obtain S. brasiliensis inoculums for experiments *in vitro*. As showed in Figure 9, between the colony forming unit count, the OD_{660nm} measurement and the Neubauer chamber count, our data show a stronger correlation between the OD_{660nm} and the colony forming unit count (R^2 = 0.91). Therefore, the number of cells in the inoculum preparation for the ATMT was calculated by the linear regression equation of the colony forming unit count and the optic density measurement.

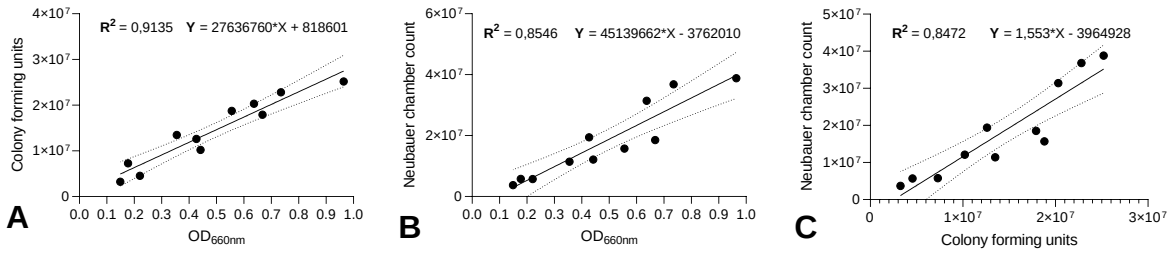

Figure 9. Differences between CFUs and Neubauer chamber count for the same OD_{660nm} measurement. Each dot represents a measurement. **(A)** Linear regression was performed between OD_{660nm} measurements and CFUs counts. **(B)** Linear regression was performed between OD_{660nm} measurements and Neubauer Chamber counts. **(C)** Linear regression was performed between CFUs and Neubauer Chamber counts.

3.3.2. *Sporothrix brasiliensis* sensitivity analysis to Hygromycin B and Chlorimuron ethyl

Our data show that *S. brasiliensis* growth inhibition in a solid medium occurred at 10^6 cells/mL with HygB concentrations at and higher than 100 μg/mL, while Sporothrix concentrations of 10^8 cells/mL were only inhibited at 250 μg/mL (Figure 10A). CE inhibit cell growth at 10 μg/mL (Figure 10B). We used the higher concentration of 150 μg/mL of HygB and 30 μg/mL of CE to avoid unspecific growth and select transformants.

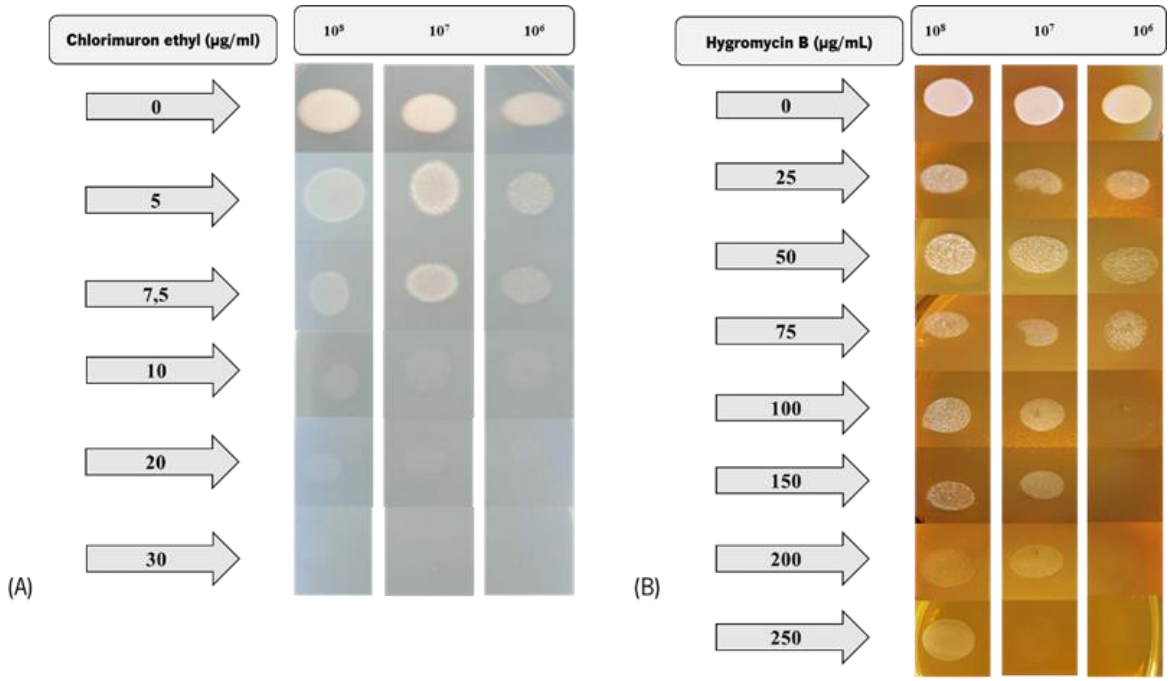

Figure 10. HygB and CE minimum inhibitory concentration of S*. brasiliensis*. Subsequent ten-fold dilutions of *S. brasiliensis* ATCC 4823 wild-type yeast cells were tested for growth inhibition at different HygB and CE concentrations (μg/mL), in YPD and YNB mediums, respectively.

3.3.3. Co-cultivation conditions influencing ATMT efficiency

To establish an ATMT protocol for *S. brasiliensis*, several co-cultivation conditions were tested, such as different *S. brasiliensis and A. tumefaciens* strains, the bacteria:fungi ratio, the type of sterile membranes used and the time of co-cultivation. The first step was to evaluate the strain which produces more transformants. The three *A. tumefaciens* strains used, LBA1100, EHA105 and AGL-1, harboring the plasmid pUR5750, showed different efficiencies during the ATMT procedure (n≥4). As shown in figure 11, when co-cultivation occurred at 26°C for 72h on Hybond™-N+ sterile membranes, there were no significant efficiency differences between strains in the 1:1 ratio of co-cultivation, only when the 2:1 ratio was applied. In this case, co-cultivation with AGL-1 showed more transformants (p=0.0001). Additionally,

AGL-1 strain efficiency was also ratio-dependent. The 2:1 ratio transformed more cells when compared to the 1:1 ratio ($p<0.0001$). Although EHA105 often showed more transformants than LBA1100 at the 2:1 ratio, it was not statistically significant.

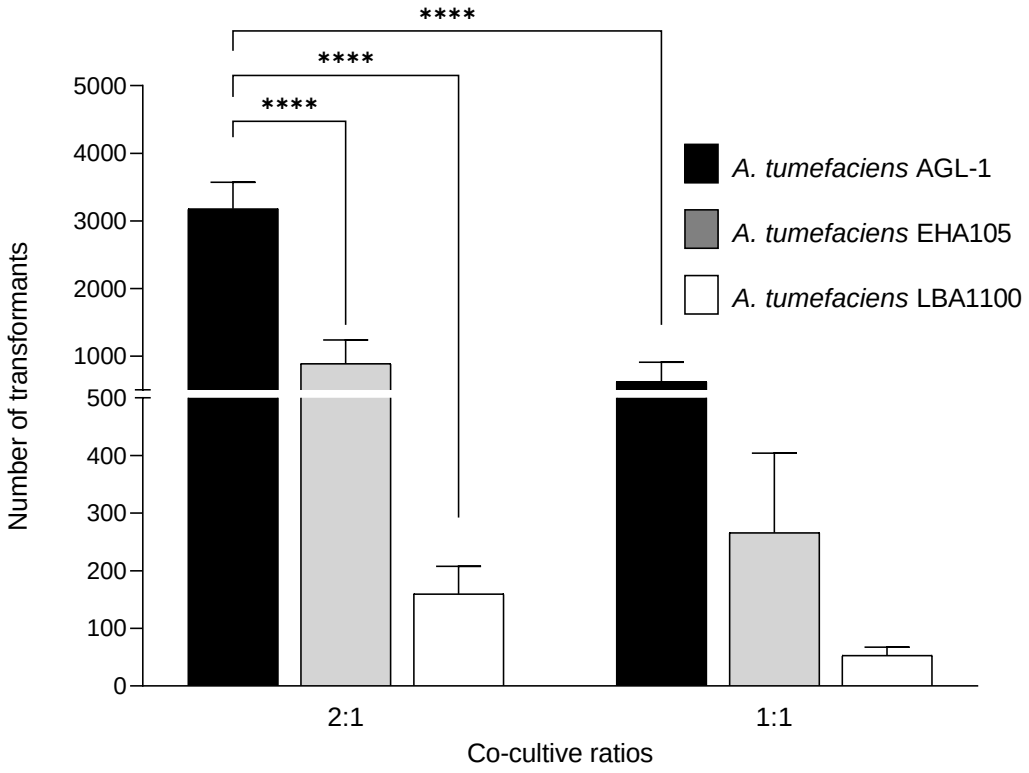

Figure 11. Effect of *Agrobacterium tumefaciens* strain (LBA11000; EHA 105 and AGL1; harboring the binary vector pUR5750) and the ratio of *Agrobacterium*:*Sporothrix* on transformation efficiency. The growing colonies on the hygromycin medium were counted as transformants. The number of transformants ± SEM per condition is represented (n ≥ 4). Statistically significant data was determined by Two-Way ANOVA by Tukey's multiple comparisons test ****($p<0.0001$).

To determine the optimal co-culture time for the ATMT of *S. brasiliensis*, four different periods (24, 48, 72 and 96h, n=6) were tested using the most efficient strain testes, AGL-1. As shown in Figure 12, fewer transformants were observed with a 24h co-cultivation time (p=0,0371). No statistical difference was observed between the 48 and 72h, and the 72 and 96 hours of co-cultivation (p =0,9368 and p=0,3129, respectively). However, 48h of co-cultivation presented more transformants than 96 hours (p=0,0121). At 72h and 96h period of co-cultivation, *S. brasiliensis* cells were able to produce sufficient biofilm (Figure 12B) to significantly impair the removal of cells from the membranes on the IM plates into the YPD medium with cefotaxime, which probably influenced and vary the number of transformants

present at the selective medium, possibly masking the true result of the ATMT efficiency for those experimental conditions.

(A)

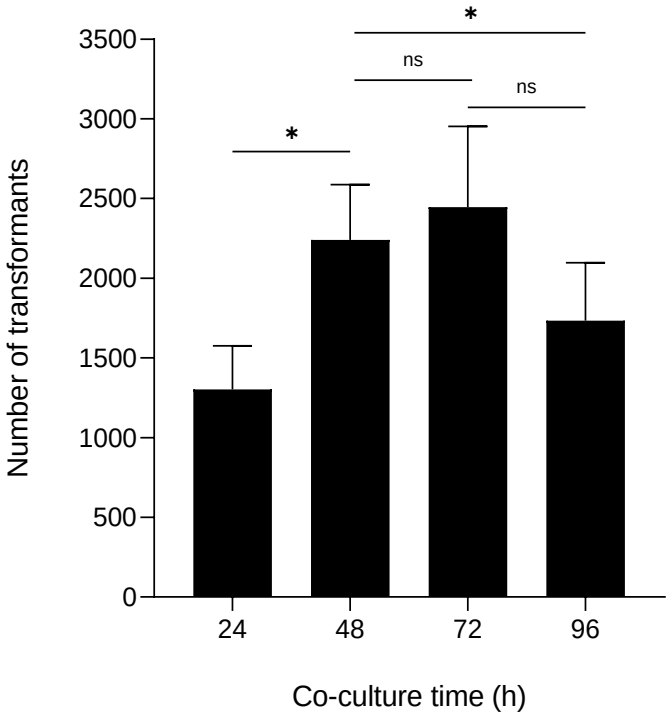

(B)

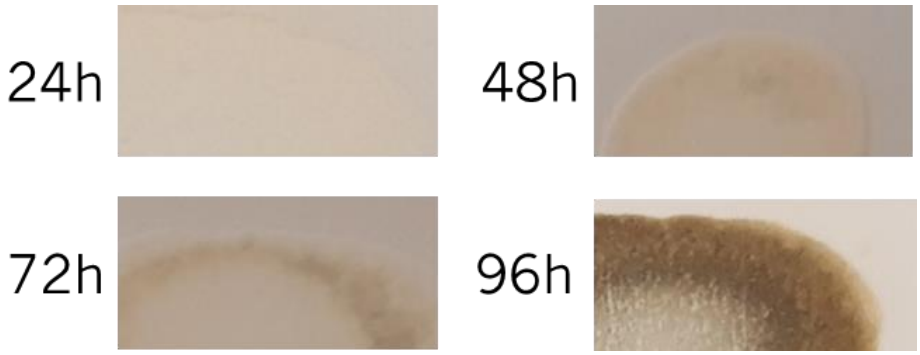

Figure 12. Effects of co-cultivation time in *S. brasiliensis* ATMT efficiency. (A) Effect of length of duration of co-cultivation on transformation efficiency. Mean values of the number of transformants ± SEM per time are represented in bars (n=6). Statistically significant data was determined by One-Way ANOVA by Tukey's multiple comparisons tests (* $p<0.05$). **(B)** Filter pieces transferred to recover medium after different co-cultivation times. (B) Filter pieces transferred to recover medium after different co-cultivation times.

In the ATMT technique, the cells can be mixed for co-cultivation above different membrane materials, such as cellophane and Hybond™-N+ (116,120) and co-cultivated at several temperatures (103,109). Only the conditions of co-cultivation with a 2:1 ratio and a co-cultivation period of 72h at 26°C were used in the comparison, due to their increased efficiency. No statistical difference was observed

between the usage of Hybond™-N+ or Hybond™-C membrane for co-cultivation (p=0,1824, Figure 13). The co-cultivation temperatures of 26°C showed more transformants (p<0.0001) and increased biofilm production than 28°C (Figure 14).

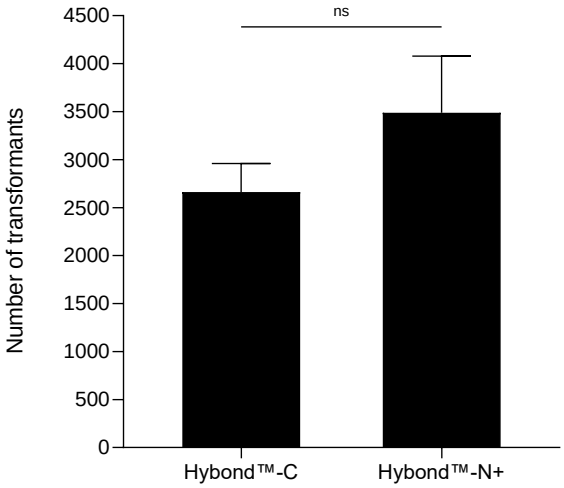

Figure 13. Effects of co-cultivation with different sterile membranes in *S. brasiliensis* ATMT efficiency. Effect on the efficiency of *S. brasiliensis* ATMT between the use of Hybond™-C or Hybond™-N+ in co-cultivation. Bars depict the mean ± SEM number of transformants per condition (n≥5). No statistical difference was observed between the membranes by the student's t-test (p=0,1496).

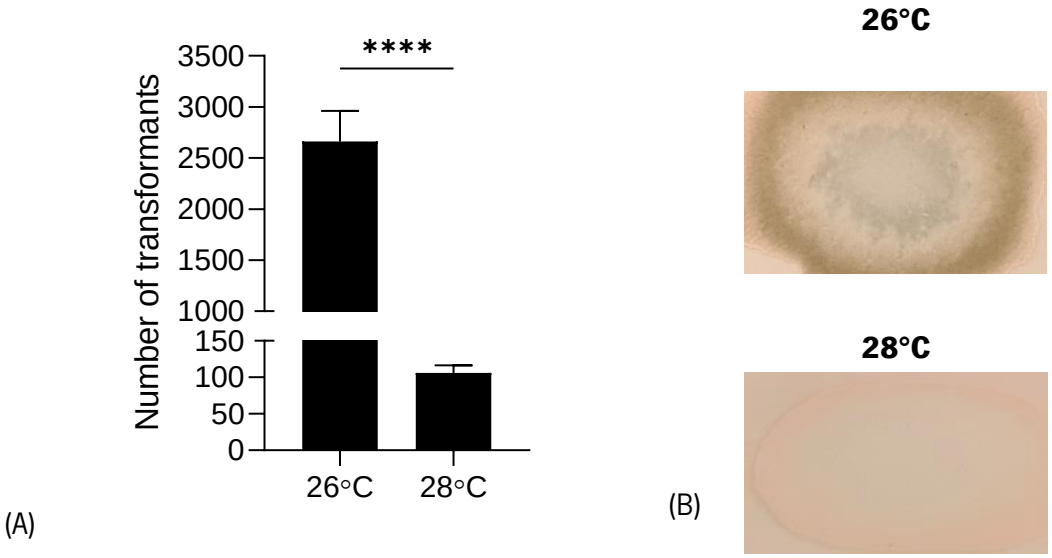

Figure 14. Effects of co-cultivation temperature in *S. brasiliensis* ATMT efficiency. (A) Effect of co-cultivation temperature in the ATMT efficiency. Bars depict the mean ± SEM number of transformants per condition (n≥10). Statistically significant data was determined by student's t-test (p<0,0001) **(B)** Filter pieces transferred to recover medium with different co-cultivation temperatures show different biofilm production.

Lastly, the efficiency of three different *S. brasiliensis* strains was compared (Figure 15). The *S. brasiliensis* strains ATCC 4823 and ATCC 4858 were able to grow rapidly both in solid and liquid mediums. However, the ATCC 4824 strain had a low growth, which difficulted the ATMT protocol, possibly impacting its efficiency. While the ATCC 4824 strain showed fewer transformants, both ATCC 4823 and ATCC4858 strains showed the same transformation efficiency (p=0,6672, n≥6). All strains had different biofilm production after 72h of incubation at 26°C.

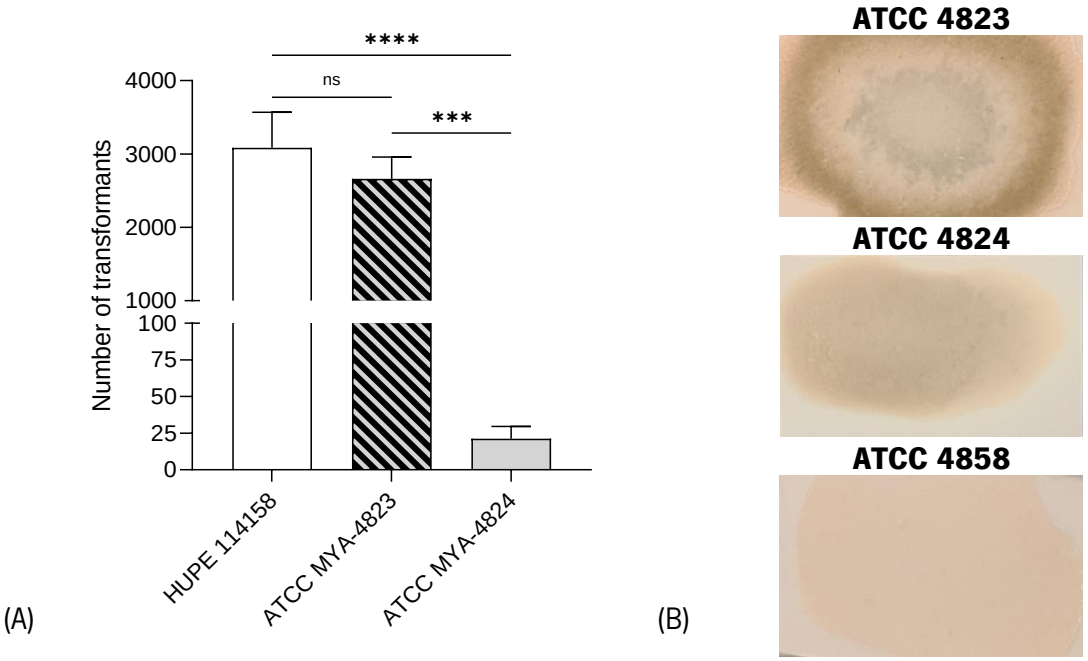

Figure 15. ATMT efficiency using different *S. brasiliensis* strains. (A) The effect of the strain *S. brasiliensis* on transformation efficiency. Bars depict the mean number of transformants ± SEM per *S. brasiliensis* strain (n ≥ 6). Statistically significant data was determined by One-Way ANOVA by Tukey's multiple comparisons tests (*p<0.05). **(B)** Filter pieces were transferred to recover medium with different *S. brasiliensis* strains, showing different biofilm production.

3.3.4. Characterization of isolated transformants

To investigate and confirm the integration of a single copy of the T-DNA into the S. brasiliensis genome after the ATMT, 5 transformants were randomly selected for DNA Extraction and subsequent qPCR analysis. DNA extraction samples ranged from 109 to 220,1ng/µL and were not contaminated. The copy numbers revealed for each of the genes closely correlated to the known copies in the genome sequence, thus confirming the validity of the described qPCR technique (Figure 16). Furthermore, transformants had a single copy of the HPH gene, thus confirming the success of the ATMT technique.

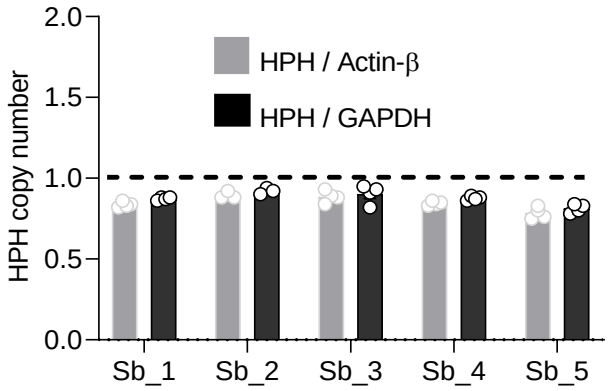

Figure 16. HPH gene screening of *S. brasiliensis* transformants via HPH copy number analysis. T-DNA copy number of *S. brasiliensis* isolates, based on glyceraldehyde-3-phosphate dehydrogenase gene (GAPDH) as a single-copy reference gene and hygromycin phosphotransferase (HPH) as a proxy for T-DNA insertion event

Isolates resistant to Chlorimuron ethyl after transformation were characterized by microscopy by the presence of the far-red Kat-fluorescence protein, TURBOFP635/Katushka. The wild-type strain, ATCC MYA-4823, showed low levels of autofluorescence, while the transformed strain expressed a sharp and bright fluorescent signal (Figure 17).

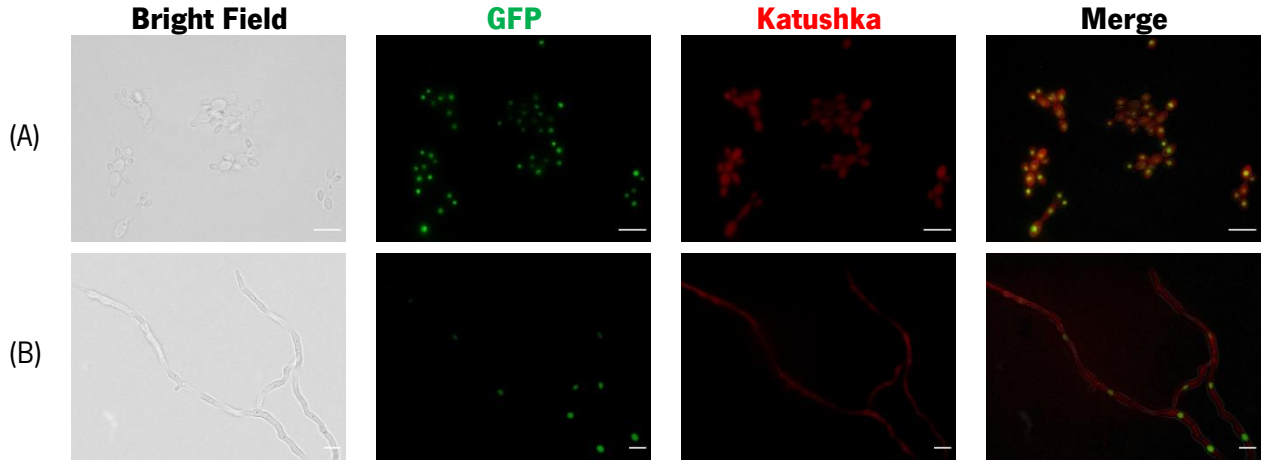

Figure 17. Fluorescence microscopic analysis of randomly-selected transformant and wild-type *S. brasiliensis* cells. The scale bar equals 10μm for all images. **(A)** Yeast cells, subsequently transformed with the plasmids pPST608::pGAPDH::H2A::GFP and pPZP201BK::SUR::gpdA::Kat::TrpC, with high levels of GFP fluorescence in the nucleus and TURBOFP635/Katushka fluorescence in the cytoplasm. **(B)** Hyphae and conidia transformants cells, subsequently transformed with the plasmids pPST608::pGAPDH::H2A::GFP and pPZP201BK::SUR::gpdA::Kat::TrpC, presented as, with high levels of GFP fluorescence in the nucleus and TURBOFP635/Katushka fluorescence in the cytoplasm.

3.3.5. Mitotic stability characterization

Transformants must be mitotically stable for an effective mutagenesis system. All five transformants presented high mitotic stability in all five generations. In five restreaks, after 12h of incubation the log (OD_{660nm}) went, on average, from 0.1 to 0.362 ± 0.032 and the mean percentage of transformant cells that expressed GFP across all generations was 99,38% ± 0.45% (Figure 18). Overall, these results suggest that 26°C for 72h of co-cultivation, using a 2:1 (bacteria:fungi) ratio is sufficient to promote the insertion of the T-DNA into the genome of *S. brasiliensis* cells yeast cells resulting in mitotically stable transformants.

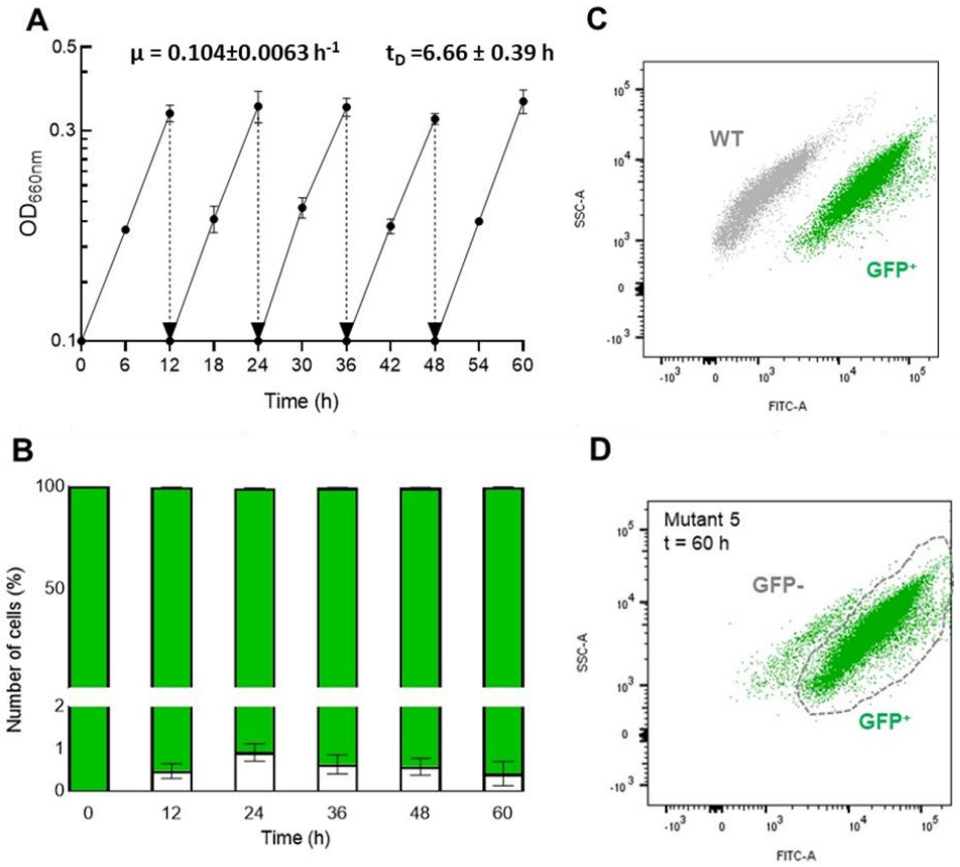

Figure 18: Mitotic stability measurement through GFP gene stability analysis. (A) Five randomly-selected transformant colonies were restreak five times in a non-selective medium. The data represent the means of log (OD_{660nm}) ± SEM after five restreaks of 12h of incubation. μ and t_d stand for the specific growth rate of the microorganism and time required for cell duplication, respectively. **(B)** Percentage of transformant cells that expressed GFP across all five generations, each one with a twelve-hour incubation period in a non-selective medium. Bars depict the mean of MFI ± SEM percentage of negative cells per restreak (n = 5). **(C)** Dot plot of side scatter (SSC-A LOG) versus green fluorescence

intensity (FITC-A), showing the higher MFI of GFP positive cells (*S. brasiliensis,* transformed with pUR5750) when compared with wild-type cells. **(D)** Representative (*S. brasiliensis,* transformed with pUR5750) dot plot of side scatter (SSC-A LOG) versus green fluorescence intensity (FITC-A) with a selective gate defined around the cellular subpopulation which is GFP positive.

3.4. Discussion and conclusion

Sporotrichosis is nowadays the most prevalent and distributed subcutaneous mycosis worldwide. The most virulent etiological agent of this disease is *S. brasiliensis*, but the virulence mechanism behind it is still unclear (50). There is yet a limited genetic manipulation tool repertoire for the *Sporothrix* genus (110), hence the development of a system for its genetic manipulation was the main goal of this work.

Agrobacterium tumefaciens-mediated transformation (ATMT) offers an efficient tool for random insertional mutagenesis and had already been performed in several different fungal species, including *Sporothrix schenckii* (89,92,98,103,116). Although ATMT has already been standardized for *S. schenckii* (98–100), besides Ferreiras' work (109), the information about the use of this technique in *S. brasiliensis* is scarce (109). Therefore, we decided to develop and establish this methodology in *S. brasiliensis*.

Several co-cultivation conditions already pre-established in other fungi were tested to evaluate their effect on *S. brasiliensis* ATMT efficiency, such as the effect of time, temperature, bacteria:fungi ratio, strains used, and type of sterile membrane used. All those variables can be of extreme importance for the transformation efficiency because they change the co-cultivation environment in which the transference of DNA from bacteria to fungal cells occurs (115).

Concerning feasibility, some co-cultivation conditions had to be based on published studies. The bacteria:fungi mixture placed in membranes was air dried for 30 min in the flow chamber before incubation according to previous work (103). Moreover, it has been reported that T-DNA can be inserted not only into protoplasts but also into intact cells by ATMT (89), including *S. schenckii* cells (98–100), which avoided the laborious protoplasts preparation process. Additionally, yeast cells were used in the co-cultivation instead of conidia, since yeasts has being reported as easily transformed using the ATMT technique (115).

The chromosomal background of the *A. tumefaciens* strain also plays an important role in the ATMT system efficiency. In addition to the function of the vir region, the recognition and binding of *A. tumefaciens* to the host surface also depends on the genes encoded in the bacterial genome (121). In addition to the *A. tumefaciens* strain, the ideal bacteria:fungi ratio depends on the transformation system and fungi species since the addition of both bacterial or fungal cells can decrease or enhance the ATMT

efficiency (115). Several experiments have proven those claims empirically, even with *S. schenckii* ATMT (92,98,116). The three *A. tumefaciens* strains used, LBA1100, EHA105 and AGL-1, harboring the plasmid pUR5750, showed different efficiencies during the ATMT procedure. However, there were no significant efficiency differences between strains in the 1:1 ratio of co-cultivation, only when the 2:1 ratio was applied. In this case, co-cultivation with AGL-1 strain showed more transformants ($p<0.0001$). This result is similar to Zhang's work (98), indicating that the strain of *A. tumefaciens* used affects the efficiency of *S. brasiliensis* transformation, where AGL-1 is the more efficient one. Although EHA105 often showed more transformants than LBA1100 at the 2:1 ratio, it was not statistically significant.

The co-cultivation time is a critical step in the transformation procedure, which varies according to *Agrobacterium* strains of and host species (122,123). Fewer transformants were observed with a 24h co-cultivation time ($p<0.0104$), as reported before (98,116,120). The incubation periods of 48h and 72h showed more transformants.

In the ATMT technique with thermos-dimorphic fungi, the cells can be mixed for co-cultivation above different membrane materials, such as cellophane and Hybond™-N+ (102,104,105,116,120). *S. schenckii* has already been transformed using both cellophane and Hybond™-N+ membranes (98,99), while the only transformation protocol for *S. brasiliensis* until this present work used the Hybond™-N+ membrane (109). No statistical differences were observed between the sterile membranes Hybond™-N+ and Hybond™-C.

The temperature is often described to affect ATMT efficiency, and optimal temperatures frequently range between 20°C and 28°C (103). ATMT protocols using *S. schenckii* were reported using the co-cultivation temperature from 25°C to 28°C (98–100) and in Ferreira's work (109), between 25°C and 27°C, the last one produced more *S. brasiliensis* transformants. The chosen temperatures to be tested were 26°C and 28°C, where the colder one produced more transformants and biofilm. Lastly, all *S. brasiliensis* strains available in the laboratory were used to compare ATMT efficiency. The *S. brasiliensis* strain ATCC MYA-4824 did not grow properly in YPD, BHI, or BD Sabouraud Glucose, which difficulted the implementation of the ATMT protocol, possibly impacting its efficiency. While the ATCC MYA-4824 strain showed few transformants, ATCC MYA-4823 and HUPE 114158 strains showed, on average, thousands of transformants, with no statistical difference between them.

Our results point to 72h of co-cultivation at 26°C, the AGL-1 strain and the 2:1 ratio (bacteria:fungi) as ideal conditions for a high number of transformants. In these conditions, we obtained 3179 ± 1171 transformants/co-cultivation. Our PCR analysis showed that all $HygB^R$ clones harboured the HPH gene.

Transformants mitotic stability is usually measured by analysing the stability of resistance gene marker used to transform the fungi. Traditionally, randomly-selected transformants are successively cultured on plates without the selective marker for three to five generations, to then be plated again with selective medium. Mitotic stability is quantified by the percentage of transformants that survive and grow in this selective medium by maintaining the resistance gene inside its genome (99,116,117,124). Our approach relied in the same principle, where mitotic stability was measured by the persistence of the GFP gene inside the genome of the pGAPDH::GFP transformants. All the selected transformants were mitotically stable.

In conclusion, the present work contributes to the implementation of an efficient ATMT protocol for the generation of a *S. brasiliensis* mutant library, a valuable asset to uncover the association between gene functions and virulence traits of this emerging and highly virulent pathogen.

CHAPTER 4

Macrophage infection and fungicidal assays with *Sporothrix brasiliensis* fluorescent strains

Abstract

Inside the *Sporothrix* pathogenic clade, *S. brasiliensis* is the most virulent species. Since the discovery of autofluorescence proteins, strains expressing GFP have become a powerful tool, which can help better understand the pathophysiology of several pathogens, including *S. brasiliensis*. Strains expressing GFP in the nucleus (H2A::GFP) and the cytoplasm (pGAPDH::GFP) created in our laboratory were used to assess their applicability as tools for the evaluation of several *in vitro* assay antifungal mechanisms of immune cells. No statistical difference in cytokine production was observed between stimulation with wildtype or pGAPDH::GFP strain. The pGAPDH::GFP strain was used to infect both PBMCs and hMDMs for 2 hours, at the MOI of 1:5. In both cases, we were able to visualize a strong GFP fluorescence inside the monocytes/macrophages, in both microscopic and FACS analysis. These results demonstrate the applicability of the pGAPDH::GFP strain in infection experiments. On the other hand, the results obtained with pGAPDH::H2A::GFP *S. brasiliensis* strain were not promising. In all the fungicidal experiments performed, this strain failed to provide a binary correlation between the loss of nucleus GFP fluorescence and loss of fungal viability or fungal death. Further experiments are required and may provide a correlation between the percentage of mean GFP intensity lost and cell viability markers. Additionally, upon monocytes/macrophages' engulfment, the GFP fluorescence from this strain became undetectable by FACS and microscopy.

4.1. Introduction

Sporotrichosis has become a public health concern as is the most prevalent subcutaneous mycosis worldwide (1). Within the *Sporothrix* pathogenic clade, the most virulent species with the most impactful clinical manifestations is *S. brasiliensis* (1,18,48–51,125). The limited repertoire of genetic manipulation tools for the *Sporothrix* genus limits the research in S. brasiliensis pathophysiology (54,110). Autofluorescent proteins, such as the green fluorescent protein (GFP), are convenient tools that assist experimentation and research with intact living cells and organisms in fields ranging from cell biology to biomedicine (126,127). Their use has already been reported on a broad spectrum of cells, such as protozoa, fungi, plants, animals, and viruses (128–132). Even though several methods to detect apoptosis are currently available, many are laborious process that often require additional use of dyes, specific substrates, enzymes, or antibodies. The use of GFP strain cells has already been used to detect the induction of apoptosis, necrosis and cytotoxicity, which can help avoid other work-intensive and resource-intensive screening procedures (133,134).

The exact role of immune cells in *Sporothrix* spp. infection is not yet fully elucidated, but macrophages are probably the most important immune cells for containing and terminating sporotrichosis (68,69) since their phagocytic activity plays a crucial role in surveillance and clearance of fungal pathogens (70,71). GFP-expressing strains have also been used to study the interaction of macrophages with bacteria and fungi (135–138). Although *S. schenckii* strains expressing GFP have already been produced (99), currently there is no report of *S. brasiliensis* strains expressing GFP, and their interaction with macrophages.

4.2. Materials and Methods

4.2.1. Ethics statement.

The functional experiments involving cells isolated from the peripheral blood of healthy volunteers at Hospital of Braga, Portugal, were approved by the Ethics Subcommittee for Life and Health Sciences (SECVS) of the University of Minho, Portugal (no. 014/015). Experiments were conducted according to the principles expressed in the Declaration of Helsinki, and participants provided written informed consent.

4.2.2. Microorganism and cell culture conditions

S. brasiliensis strains expressing GFP in the cytoplasm (pGAPDH::GFP, Figure 19A) and the nucleus (pGAPDH::H2A::GFP, Figure 19B) were designed and produced in the lab by collaborators (Table 3). To that end, plasmid DNA extraction, recombinant DNA manipulation and *E. coli* and *A. tumefaciens* transformation procedures were performed as reported elsewhere (139,140). *S. brasiliensis* strains expressing GFP were produced through the ATMT protocol established in the previous chapter. All *S. brasiliensis* strains used in this chapter were cultured at 37°C in a selective YPD (pH = 7.8) medium with HygB (150 μg/mL), thus ensuring the presence of the GFP gene. All cultures were maintained at 4°C for short-term storage and were routinely sub-cultured every 4–6 weeks. Exponential growth yeast cells were obtained through sterile gaze filtration after a 24h incubation at 37°C in a selective YPD medium (pH = 7.8).

Table 3. Table explaining the details from both *S. brasiliensis* GFP strains used in this thesis.

Mutant name	Fluorescence	Promotor	Region of expression	Origin
pGAPDH::GFP	GFP	pGAPDH	Nucleus	Figure 19a
pGAPDP::H2A::GFP	GFP	pGAPDH	Cytoplasm	Figure 19b

(A) 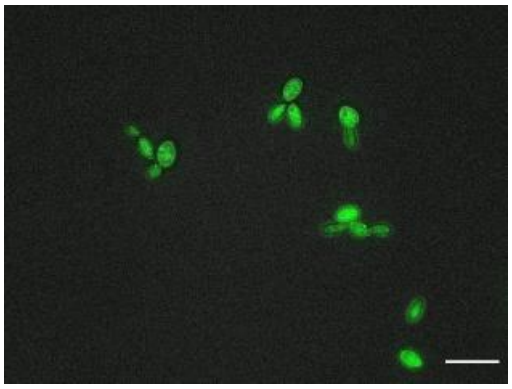 (B) 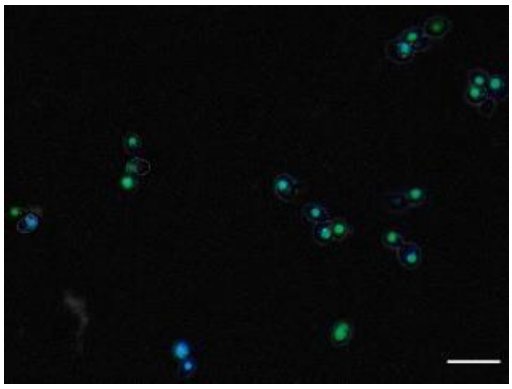

Figure 19. *S. brasiliensis* strains expressing GFP. Bright-field and FITC and DAPI channels were captured and merged with the Olympus Widefield Upright Microscope BX61, by either bright-field or fluorescent microscopy. The scale bar equals 10µm for both images. **(A)** Yeast pGAPDH::GFP cells expressing GFP in the cytoplasm with high levels of FITC fluorescence. **(B)** Yeast cells from the pGAPDH::H2A::GFP strain expressing GFP in the nucleus with high levels of FITC fluorescence. The nucleus was stained with 0.1µg/mL of Invitrogen™ DAPI and colocalization was observed.

Several steps were required to obtain human peripheral blood mononuclear cells (PBMCs) and human macrophages (hMDMs). Firstly, a 50mL falcons containing 15mL of Histopaque®- 1077 (Sigma-Aldrich) got 15mL of blood received from healthy donors slowly poured against the wall over the histopaque (1 blood: 1 histopaque). The falcons with the solution were centrifuged 400 x g for 30 min, with acceleration 3 and deceleration 1, and the serum was removed. After that, the ring of PBMCs is removed and distributed to 4 falcons of 15mL. These falcons are then washed with sterile commercial PBS (1x, Thermo Fisher Scientific), by filling them with the solution, centrifuging at 250 x g for 10 min, with acceleration 9 and deceleration 9, and carefully discarding the supernatant. After a cellular suspension of the 4 falcons in only 2 falcons (2-4 mL maximum per falcon) with sterile commercial PBS (1x), the remaining falcons are filled with red blood cells lysis buffer (155mM NH_4Cl, 10mM $KHCO_3$, 0.1mM EDTA, pH 7.3) and inverted gently. The solution is centrifuged at 250 x g for 10 min, with acceleration 9 and deceleration 9, the supernatant is carefully discarded, and the pellet is resuspended again in sterile and commercial PBS (1x). Both cellular suspensions are joined in only one falcon, the solution is washed again, and the PBMCs are counted using a Neubauer chamber. Lastly, the PBMCs were poured inside 24-well cell culture plates (SPL Life Sciences, Pocheon-si, Korea) with 500µL of cRPMI 1640 medium (Thermo Fisher Scientific) and infected with pGAPDH::GFP *S. brasiliensis* yeast cells.

To obtain human macrophages, PBMCs were acquired using the same protocol described above. After the Neubauer chamber count, the volume necessary to obtain 100 x 10^6 cells is distributed to an Eppendorfs, which is centrifuged at 2000 rpm for 5 min. The supernatant is discarded, the pellet is resuspended in 400µL of sterile MACS buffer (DPBS solution with 0.5% BSA, 2 mM EDTA, pH 7.2) and

25µL of CD14 Microbeads (Miltenyi Biotec®) per Eppendorf was added. After incubation at 4°C for 30 min, their content is transferred to 15 mL falcons, and 5 mL MACS buffer is added to wash as the solution is centrifuged at 300 x g for 10 min, supernatant is removed and the pellet is resuspended in 500µL of MACS buffer. MACS® columns (Miltenyi Biotec®) are used to isolate monocytes by passing the volume of 2 falcons per column (200 x 10^6 cells/column, maximum). Each column is washed 3 times with 500µL of MACS buffer, thus removing non-CD14 cells. Each column then is placed inside 15mL falcons, 1mL of MACS buffer is added and the volume inside each column is pressed with a syringe to be poured from the column into the falcon. Lastly, after a Neubauer chamber count, monocytes are primarily obtained by culturing the cells in a cRPMI-1640 medium in a concentration of 1x10^6 cells/mL with 20ng/mL of GM-CSF. Cells were maintained at 37°C in an incubator in a humidified atmosphere with 5% CO_2. The culture medium was renewed every three days for seven days.

4.2.3. Analysis of the correlation between loss of GFP fluorescence and cell death

To analyse the correlation between the loss of GFP fluorescence and cell death, several fungicidal experiments were performed with the *S. brasiliensis* ATCC 4823 strain pGAPDH::H2A::GFP (Figure 17b), which confers the expression of the fluorescence proteins GFP in the nucleus (Table 3). The first step was to evaluate the macrophage fungicidal activity in this strain as well as to correlate the loss of GFP fluorescence and cell death. Then, heat-fungicidal and ultra-violet-fungicidal assays were also performed for a proper interpretation of the result from the macrophage-fungicidal experiments. The protocol for each assay will be further described below, but all had the same evaluation methods, besides some minor alterations.

After each period of incubation, at each condition, a portion of cells was fixed with paraformaldehyde at a concentration of 2% for 15 minutes at 4°C and five thousand events were captured using Fluorescence-activated cell sorting (FACS). The wild-type MFI was used to determine the MFI autofluorescence threshold, and consequently the percentage of population cells that did not express GFP after each incubation period, as illustrated in Figure 20. Lastly, each condition had its number of cells measured by plating a 1:10000 dilution in a YPD (pH 7.8) solid medium, both before and after the fungicidal assay.

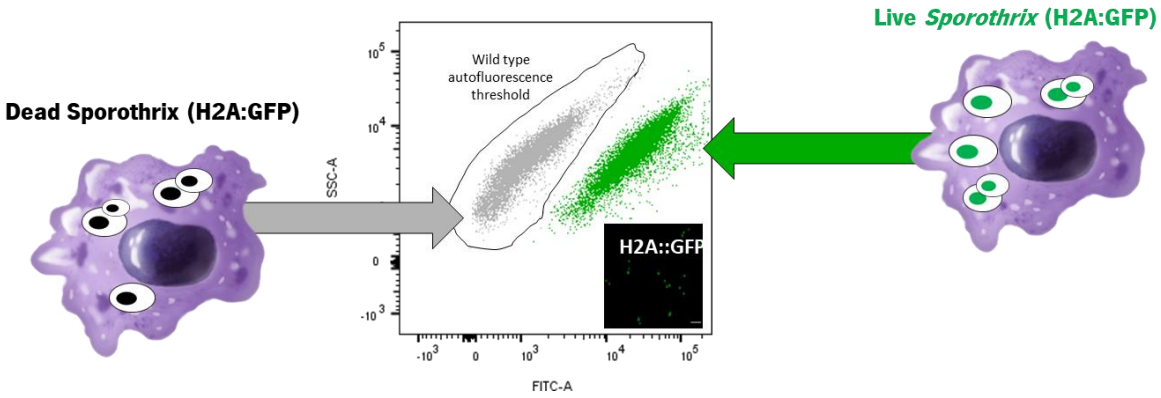

Figure 20. Schematic of *S. brasiliensis* pGAPDH::H2A::GFP loss of GFP fluorescence upon cell death. The dot plot of side scatter (SSC-A LOG) versus green fluorescence intensity (FITC-A) shows the higher MFI of GFP positive cells (pGAPDH::H2A::GFP) when compared with wild-type cells. In the lower right area of the graph, there is a microscopic image of the *S. brasiliensis* pGAPDH::H2A::GFP. Upon cell death, it is hypothesised that pGAPDH::H2A::GFP strain would lose the GFP in the nucleus, shifting the population towards the wild-type autofluorescence threshold inside the dot plot.

4.2.3.1.Macrophage-fungicidal experiments

Exponential growth yeast cells of *S. brasiliensis* pGAPDH::H2A::GFP were filtered with sterile gauze and stained with Alexa Fluor™ 647 for 40 minutes at RT while shaking and covered with aluminium foil. They were used to infect 48-well cell culture plates (SPL Life Sciences, Pocheon-si, Korea) with 250µL of cDMEM and 2.5 x 10^4 cells per well. To achieve an MOI of 10:1, each well was infected with 20µL containing 2.5 x 10^3 cells. Yeast cells were counted using Neubauer chambers with Ten-fold dilutions using Trypan Blue (1:10) (Gibco, California, USA), to also considerate fungal viability. Although *Sporothrix* spp yeast cells are prone to group, cell clusters where not counted as single cells and each cell was counted individually.

The inoculum was diluted to 1:500 and plated in YPD (pH 7.8) solid medium. After infection, plates were briefly centrifuged, allowing the fungus to be moved near the macrophages, and incubated at 4°C for 30 minutes, lowering PBMC metabolic and effector activities, assuring phagocytosis started simultaneously during the incubation periods at 37°C, 5% CO_2. After the incubation period of 1h, supernatants were removed, 250µL of cDMEM was added per well, and another incubation occurred, at 37°C, with 5% CO_2 for 2h. After the fungicidal protocol, plates were analysed either microscopically or using FACS.

To analyse microscopically, plates had their supernatant removed, were washed with PBS, stained with 100µL of calcofluor-white (CFW, 0.1mg/mL, Sigma-Aldrich, 10 minutes at RT) to allow the visualization of fungi adhered to the macrophage cell membrane, and fixed with 110µL of Formalin 10% for 10 minutes. Fluorescence microscopy analyses were performed with the Olympus Widefield Upright

Microscope BX61, by either bright-field (upper panel) or fluorescent microscopy (lower panels). All images were captured using 395nm/509nm for excitation and emission, respectively, and exposition time to the laser beam was automatically set. All images were captured using 395nm/509nm for excitation and emission, respectively, and exposition time to the laser beam was automatically set. Images were treated in the ImageJ© v1.8 software (https://imagej.nih.gov/ij/).

In the second technique, the plate was frozen at -80°C overnight and thawed at 37°C, 5% CO_2 for 30 min, to disrupt macrophage cell membranes and liberate yeast cells to the supernatant. 150µL of each well was stained with 3µL of PI (50ng/mL) and analysed in FACS, while the lasting 100µL was 10-fold diluted and plated in YPD (pH 7.8) solid plates. The percentage of population cells that did not express GFP and the PI-positive population were measured in FACS and compared with the relative fungicidal percentage from the CFU counted in the YPD (pH 7.8) solid plates after incubation at 37°C for 7 days.

4.2.3.2.Heat-fungicidal experiments

Exponential growth cells were acquired through culture at 37°C for 24h in a liquid YPD (pH 7.8) medium and sterile gaze filtration. The concentration of cells was adjusted by OD_{660nm} to 10^7 cells/mL per condition. Two assays with different techniques were used to evaluate the correlation between loss of GFP fluorescence and cell death on heat-fungicidal experiments.

To perform the heat-fungicidal assay at 50°C, 50 ml of YPD (pH 7.8) containing GAPDH::GFP::H2A cells at the concentration of 10^7 yeast cells/mL were poured into a 250 ml Erlenmeyer flask and incubated in an incubator shaker at 50°C for 180 minutes. At the incubation periods of zero, 60, 120 and 180 minutes, cells were fixed and analysed using FACS. Each sample was diluted and plated, both before and after the fungicidal assay, as described priorly.

To perform the heat-fungicidal assay at 65, 75 and 85°C, microtubes with 2mL of Phosphate-buffered saline (PBS) with 10^7 yeast cells/mL of *S. brasiliensis* pGAPDH::H2A::GFP strains were incubated in a thermoblock at 65, 75 and 85°C for 30 minutes. At the incubation periods of zero, 10, 20 and 30 minutes, cells were fixed and analysed using FACS. Each sample was also diluted and plated, both before and after the fungicidal assay, as described priorly.

4.2.3.3.Ultra-violet-fungicidal experiments

Exponential growth cells were acquired through culture at 37°C for 24h in a liquid YPD (pH 7.8) medium and sterile gaze filtration. The concentration of cells was adjusted by OD_{660nm} to 10^7 cells/mL per condition. To perform this assay, *S. brasiliensis* yeasts expressing GFP in the nucleus

(pGAPDH::H2A::GFP) at a concentration of 10^7 cells/mL were cultured in Petri dishes with 15mL of Phosphate-buffered saline (PBS) with a spinning magnet to promote shaking inside a safe cabinet with the UV lamp turned on. The plates had their cover removed and were positioned near the UV lamps, radiating light at a wavelength of 254 nm (UV-C band), to promote proper DNA damage and cellular apoptosis. At the incubation periods of zero, 60, 120, 180 and 240 minutes, cells were fixed and analysed using FACS. Each sample was diluted and plated, both before and after the fungicidal assay, as described priorly.

4.2.4. Cytokines production assays

To compare the cytokines production between PBMCs and hMDMs upon infection with wildtype and pGAPDH::GFP *S. brasiliensis* cells, exponential growth yeast cells were filtered, washed with PBS, counted, and resuspended to the desired infecting concentration in 20µL of PBS. Cells were counted using Neubauer chambers with Ten-fold dilutions using Trypan Blue (1:10) (Gibco, California, USA), to also considerate fungal viability. Although *Sporothrix* spp yeast cells are prone to group, cell clusters where not counted as single cells and each cell was counted individually. To achieve MOI of 1:10, each well containing 0.5 x 10^6 macrophages/monocytes was infected with 5 x 10^6 yeast cells in a 24-well plate (SPL Life Sciences, South Korea). After infection, plates were briefly centrifuged, allowing the fungus to get close to the macrophages/PBMCs, and incubated at 4°C for 30 minutes, lowering macrophage and PBMCs metabolic and effector activities, promoting phagocytosis. Cells were incubated at 37°C, 5% CO_2, for 20h. After incubation, supernatants were collected and stored at -20°C for cytokine measurements.

Cytokines were measured with the LEGENDplex™ Human Macrophage/Microglia Panel (13-plex, BioLegend®, USA), following the manufacturer's instructions. Briefly, samples were incubated with the fluorescent beads and incubated for 2h at room temperature. After incubation, beads were washed through centrifugation and addition of wash buffer. Then a cocktail of detection antibodies was added to the beads, following an incubation of 1h. After incubation, the subtract Streptavidin-PE (SA-PE) was added to bind to the detection antibodies and beads were incubated for 30minutes. After incubation, beads were washed again and resuspended in wash buffer. The data from each sample were acquired on LSRII flow cytometer (BD Biosciences) using DIVA software and data was analyzed using the BioLegend's LEGENDplex™ Data Analysis Software©.

4.2.5. Phagocytosis assays

Exponential growth yeast cells of *S. brasiliensis* pGAPDH::GFP were used to infect, PBMCs and human macrophages (hMDMs) in 24 or 48-well cell culture plates (SPL Life Sciences, South Korea). Yeast cells were filtered, washed with PBS, counted, suspended, and strained with CFW (0.1mg/mL, Sigma-Aldrich, 30 minutes at RT while shaking). After that, they were washed three times with PBS X1 and resuspended to the desired infecting concentration in 20µL of PBS. Cells were counted using Neubauer chambers with Ten-fold dilutions using Trypan Blue (1:10) (Gibco, California, USA), to also considerate fungal viability. Although *Sporothrix* spp yeast cells are prone to group, cell clusters where not counted as single cells and each cell was counted individually. To achieve MOI of 1:5, each well containing 0.5 x 10^6 cell was infected with 20µL containing 2.5 x 10^6 yeast cells. The inoculum was also diluted to 1:500 and plated in YPD (pH 7.8) solid medium. After infection, plates were briefly centrifuged, allowing the fungus to be pushed near the macrophages, and incubated at 4°C for 30 minutes, lowering cell metabolic and effector activities, assuring phagocytosis started simultaneously during the incubation periods at 37°C, 5% CO_2. Phagocytosis occurred for 2h at 37°C, with 5% CO_2.

To perform the FACS analysis, plates had their supernatant removed, were washed with PBS, and incubated with 250µL of Accutase™ (GRiSP, Portugal) at 37°C for 10 minutes. Cells were then dislodged with a pipette into a 96-well u-shaped cell culture plate and stained with Brilliant Violet 650™ anti-human CD14 Antibody (Biolegend®, USA) for 10 minutes at room temperature. Plates had their supernatant removed, 100µL of PBS was added and cells were analyzed in FACS, as illustrated by the gate strategy in Figure 21.

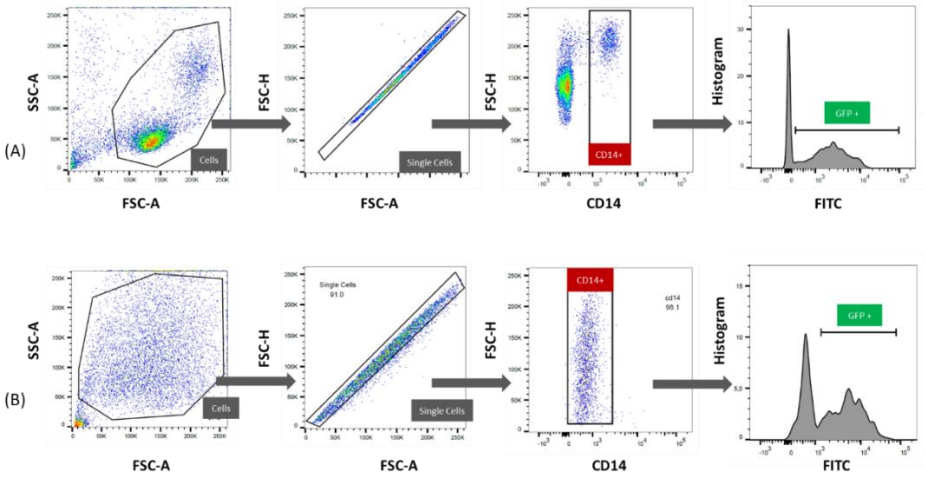

Figure 21. Schematic of the gating strategy used to analyse phagocytosis in FACS. (A) Gating strategy used to analyse phagocytosis in PBMCs. **(B)** Gating strategy used to analyse phagocytosis in hMDMs.

To perform the microscopic phagocytosis analysis, plates had their supernatant removed, were washed with PBS and each well had the number of internalized fungi inside macrophages counted using the Olympus Widefield Upright Microscope BX61, by either bright-field (upper panel) or fluorescent microscopy (lower panels). All images were captured using 395nm/509nm for excitation and emission, respectively, and exposition time to the laser beam was automatically set. Images were treated in the ImageJ© v1.8 software (https://imagej.nih.gov/ij/). The percentage of phagocytosis was measured based on the GFP fluorescence of the pGAPDH::GFP strain and according to this subsequent formula:

$$\textbf{Phagocytosis } \% = \left(\frac{\text{number of Monocytes/macrophages with internalized yeast}}{\text{number of Monocytes/Macrophages in the same field}}\right) \text{X } 100\%$$

An additional step was performed in the infection protocol of macrophages. To measure the number of adhered yeast to the macrophage cell membrane, each well was stained with calcofluor (CFW, 0.1mg/mL, Sigma-Aldrich, 10 minutes at RT) before the infection period. Lastly, the percentage of adhered yeast cells was compared to the total amount of macrophages, by FACS and microscopy.

4.2.6. Statistical analysis

Data from the evaluation of phagocytosis indexes and fungicidal activities were obtained on a BD FACS LSRII instrument (B.D. Biosciences) and an Olympus Widefield Upright Microscope BX61. Data were processed using FlowJo® v.10 software (Tree Star Inc., https://www.flowjo.com/) and ImageJ® v.1.8 software (https://imagej.nih.gov/ij/)**.** Data are reported as the mean ± standard error of the mean (SEM) of at least two independent assays with two or three replicates. The statistical analysis was performed using GraphPad Prism Software version 8.0 (GraphPad Software Inc, USA, https://www.graphpad.com/scientific-software/prism/). The normality assumptions were assessed in all cases using the Shapiro-Wilk test. Comparing phagocytosis indexes and the percentage of dead cells upon fungicidal experiments were made by either One-Way ANOVA or Two-Way ANOVA. Statistically significant values are indicated as follows: *p ≤ 0.05, **p ≤ 0.01, ***p ≤ 0.001 and ****p ≤ 0.0001.

4.3. Results

4.3.1. Analysis of the correlation between loss of GFP fluorescence and cell death

Microscopic analysis showed that, upon phagocytosis, the pGAPDH::H2A::GFP fluorescence intensity was not strong enough to be distinguish from the macrophages autofluorescence (data not shown). Additionally, after 1 hour of phagocytosis and 2 hours of fungicidal activity, three cell death

parameters were compared (Figure 22). Even though 73.24 ± 7.27% of the cells still had their GFP fluorescence, only 45.11 ±12.38% of them were alive (PI-negative). Additionally, from an inoculum containing 4,625 x 10^4 yeast cells, only 23.96 ± 2.154% of cells appeared as CFU in the YPD plates after the fungicidal procedure, despite 73.24± 7.27% of them still had a GFP-fluorescence above the wildtype autofluorescence threshold. These results demonstrated that the loss of cell viability or cell death does not correlate with the loss of GFP fluorescence while using the pGAPDH::H2A::GFP *S. brasiliensis* strain. Further fungicidal assays were performed to evaluate this hypothesis.

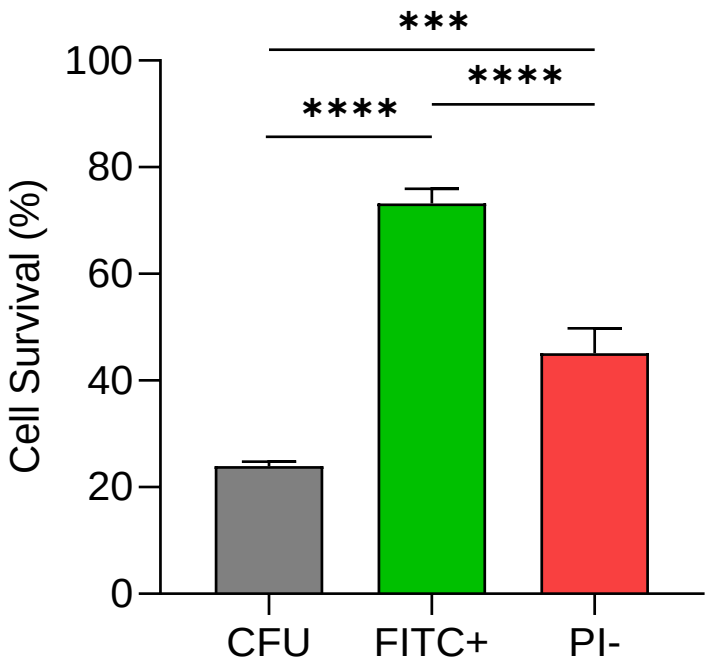

Figure 22: Analysis of the correlation between loss of GFP fluorescence and cell death by Macrophage-fungicidal assay. The PI-negative bar depicts the percentage of cell survival ± SEM (n=7). The FITC positive bar shows the percentage of cells ± SEM which express GFP fluorescence (n=7). The CFU bar represents the percentage of CFU ± SEM present in the plated YPD medium (n=7). Statistically significant data was determined by One-Way ANOVA by Tukey's multiple comparisons test.

As shown in Figure 23, in fungicidal assays with ultraviolet radiation and incubation with high temperatures, the promotion of cell death once again did not correlate with the loss of GFP fluorescence by pGAPDH::H2A::GFP *S. brasiliensis* strain. When those cells were submitted to the incubation temperatures of 50 and 65°C and ultraviolet radiation, although no CFU was present in the YPD plates, meaning cells were no longer viable, at least 95% of those cells still had the GFP fluorescence beyond the wild-type autofluorescence threshold. Even after incubation of 30 minutes with the higher temperatures

of 75 and 85°C, at least 11 and 7% of cells respectively still emitted a GFP fluorescence intensity above the wild-type autofluorescence threshold while no CFU was present in the YPD plates.

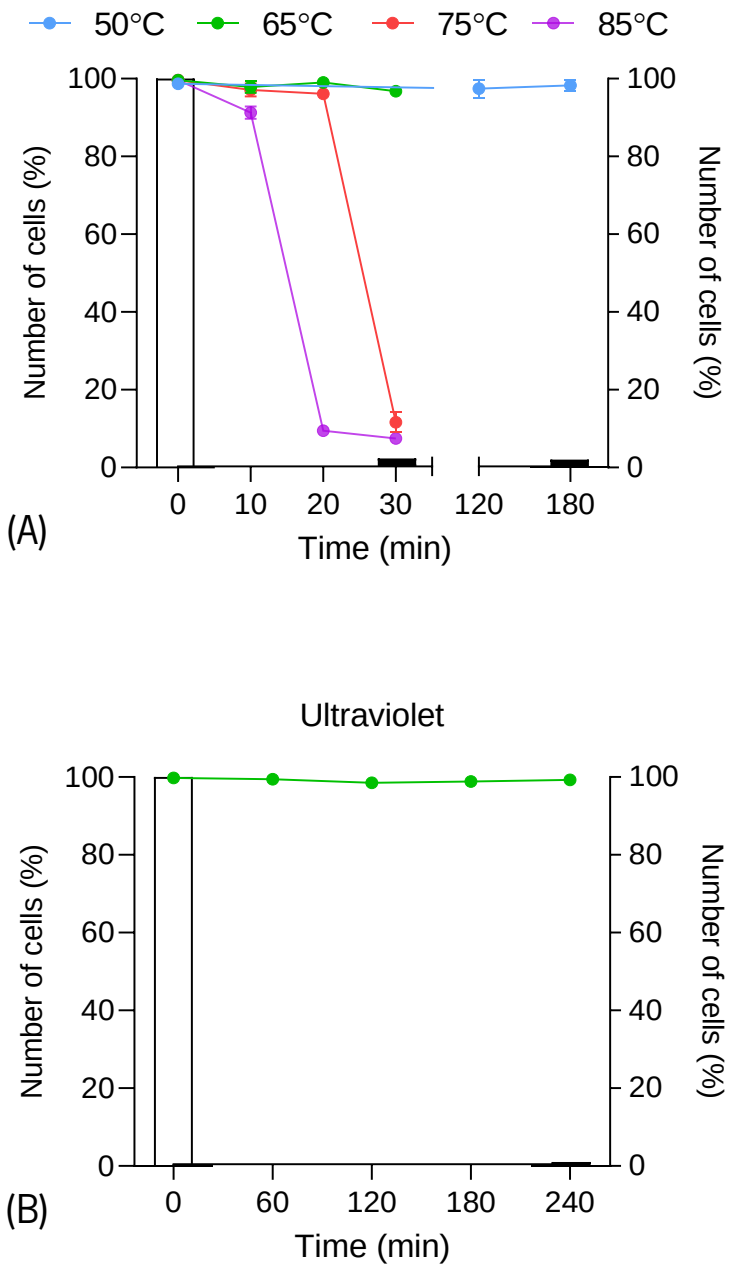

Figure 23: Analysis of the correlation between loss of GFP fluorescence and cell death by Heat-fungicidal assay. The pGAPDH::H2A::GFP *S. brasiliensis* strain was used in all assays. **(A)** Analysis of the correlation between loss of GFP fluorescence and cell death by several heat fungicidal assays. Bars depict the percentage of yeast cells present in the plated YPD medium before (white bar, at the left y axis) and after (black bars, at the right y axis) 30 and 180 minutes of incubation (n=4). Dots represent the percentage of cells that expressed GFP fluorescence throughout the incubation periods, for each incubation temperature (n=4). **(B)** Analysis of the correlation between loss of GFP fluorescence and cell

death by Ultraviolet-killing. Bars depict the percentage of cells present in the plated YPD medium before (white) and after (black) the U.V. radiation (n≥4). Green dots represent the percentage of cells that expressed GFP fluorescence throughout the same period (n≥4).

4.3.2. Cytokines measurement

The production of pro and anti-inflammatory cytokines in human PBMCs were evaluated after 24h of exposure to yeasts of wild-type and pGAPDH::GFP *S. brasiliensis* cells. As demonstrated in Figure 24A, B and C, the levels of TNF, IL-6 and IL-10 was higher in stimulated wells ($p \leq 0.05$), regardless of the fungal strains used, wildtype or pGAPDH::GFP. No statistical difference in cytokine production was observed between stimulation with wildtype or pGAPDH::GFP yeast cells in those three cytokines.

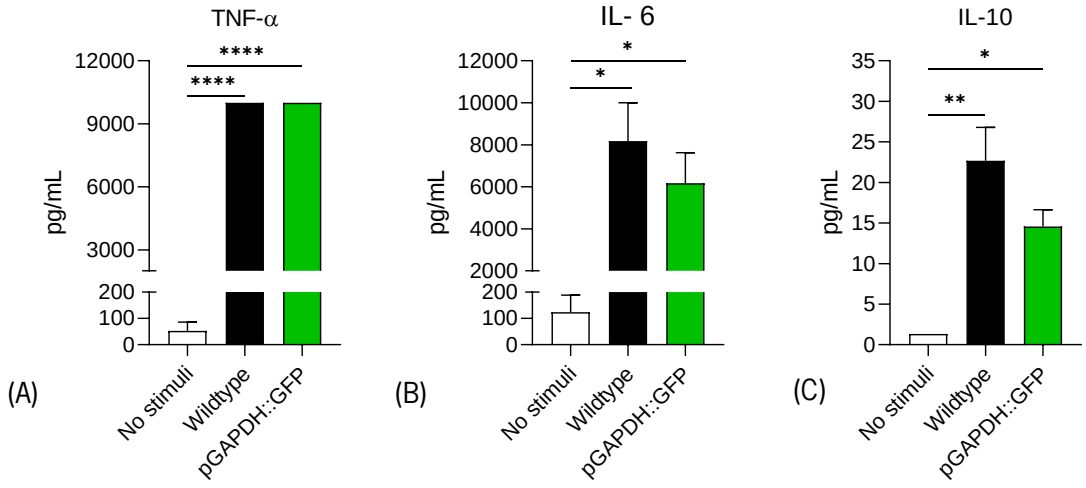

Figure 24. Stimulation of PBMCs with *S. brasiliensis* wild-type and pGAPDH::GFP cells results in high production of cytokines. Bars depict the concentration of TNF-α (A), IL-6 (B) and IL-10 (C) after 20h of stimulation with wild-type (black) and pGAPDH::GFP (green) cells. The data were expressed as mean ± SEM. Statistically significant data was determined by One-Way ANOVA by Tukey's multiple comparisons test (n≥3).

4.3.3. Phagocytosis analysis using the pGAPDH::GFP strain

The GFP fluorescence of the pGAPDH::GFP strain was used as parameter to measure the percentage of phagocytosis in the infection assays with PBMCs and hMDMs. Infection occurred for two hours in a MOI of 1:5. Analysing by FACS, the percentage of phagocytosis with CD14+ PBMCs was 56.18 ± 1.78%, and 61.48 ± 4.32% with hMDM. Analysing by microscopy, the percentage of phagocytosis of PBMCs (CD14+) and hMDM were, respectively, 54.83 ± 2.20 and 64.25 ± 4.07. No statistical difference was observed between the percentage of phagocytosis (n≥6, Two-Way ANOVA by Tukey's multiple

comparisons test), as depicted in Figure 25A. Furthermore, pGAPDH::GFP *S. brasiliensis* cells exhibited a strong GFP autofluorescence upon phagocytes engulfment (Figure 25B, C).

Only in the hMDM infection protocol, calcofluor-white was used post-infection to stain the fungal cell adhered to the macrophages' cell membrane. In that case, the percentage yeast cells adhered was 9.34 ± 2.42% and 6.39 ± 1.90%, according to the FACS and microscopic analysis, respectively (Figure 25D). Figure 25C illustrates the blue layer (CFW staining) overlaying with the FITC layer, revealing the non-phagocytosed but adhered yeast cells.

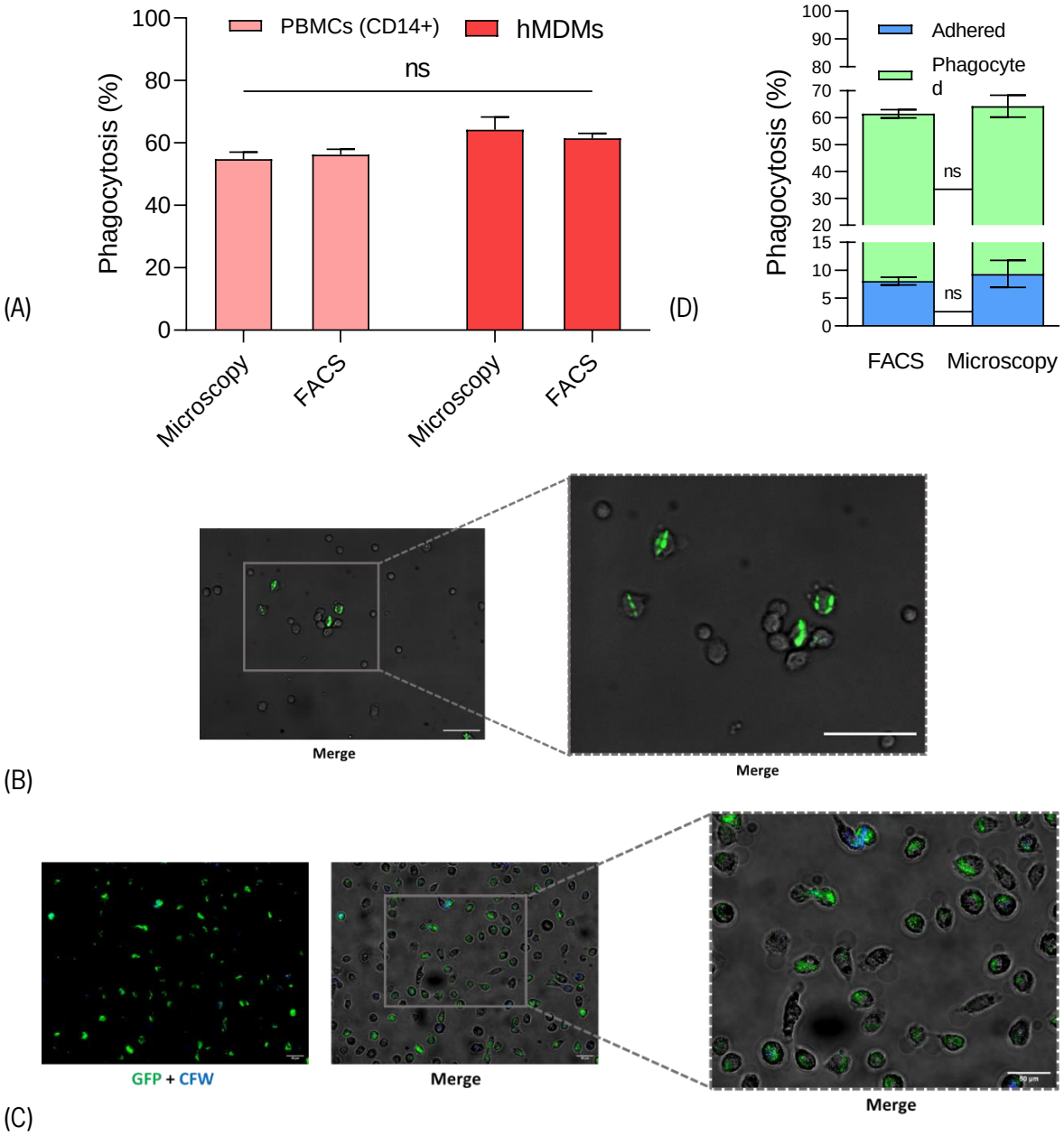

Figure 25. Phagocytosis assay analysis using *S. brasiliensis* pGAPDH::GFP strain to infect PBMCs and hMDMs.

(A) Comparison of phagocytosis between human monocytes and macrophages of *S. brasiliensis* pGAPDH::GFP yeast cells at

the MOI of 1:5. Both FACS and microscopic techniques to count phagocytosis were compared. Bars depict the percentage of phagocytosis ± SEM (n≥6). No statistical difference was observed. **(B)** The green layer and bright fields were merged to visualize GFP fluorescence of the pGAPDH::GFP strain inside cd14+ PBMCs. **(C)** Blue layer (CFW staining) overlaid with the FITC layer revealing the difference between phagocytosed and non-phagocytosed but adhered yeats. **(D)** Percentage of phagocytosis obtained by infecting hMDM at an MOI of 1:5 for 2 hours. The green bars depict the mean percentage ± SEM of internalized/adhered GFP-expressing yeast cells, while the blue bars show the mean percentage ± SEM of adhered cells within the GFP-positive macrophages, relative to the total macrophage population. Internalization and adherence percentages are compared between from FACS and microscopy analyses. Scale bars equal 50 μm for all images.

4.4. Discussion and conclusion

Several fungicidal assays evaluated the loss of cell viability or cell death with the loss of GFP fluorescence of the pGAPDH::H2A::GFP *S. brasiliensis* cells (nucleus GFP expression). Firstly, the fungicidal assay performed with hMDMs failed make this correlation (Figure 22), thus requiring further inquiry. With that in mind, fungicidal experiments by incubation high temperatures were realized and failed to demonstrate a correlation between the loss of GFP fluorescence and cell viability (Figure 23). Despite all of them having no cell viability after the incubation period at 50 and 65°C, the GFP fluorescence was still present. Only in the higher temperatures of 75 and 85°C, which are known to cause GFP denaturation (141), the GFP fluorescence decayed. Since the DNA is main molecule damaged by ultraviolet radiation (142,143), pGAPDH::H2A::GFP cells were submitted to this radiation in a fungicidal assay, to confirm if the MFI decayed due to the protein denaturation instead of the loss of cell viability. The results were like the fungicidal assays by temperatures of 50 and 65°C, meaning cell viability was completely impaired while GFP still emitted fluorescence. These results corroborate with authors who claim the GFP may not show a significant difference between live and apoptotic populations, thus requiring a multiparametric assay for a more precise interpretation of cell viability (144). Perhaps, a thorough analysis could correlate the percentage of mean GFP intensity lost with cell viability markers (133,134), instead of the binary approach used in the gating strategy of the FACS in this thesis. Nevertheless, the GFP expression of pGAPDH::H2A::GFP strain was not intense enough to be distinguished from the macrophages/monocytes autofluorescence, which makes both the accounting of the phagocytosis index and the binary analysis of cell death not viable for this strain.

S. brasiliensis pGAPDH::GFP yeasts (cytosolic GFP expression), were used to analyse phagocytosis. However, there is a small change the random insertion site of the Ti DNA inside the genome can alter the microorganism virulence and immunological interaction with the host (145). To evaluate that, the production of cytokines in human PBMCs were compared after 24h of exposure to yeasts of

wild-type and pGAPDH::GFP *S. brasiliensis* cells. As demonstrated in Figure 23, no statistical difference in cytokine production was observed between stimulation with wildtype or pGAPDH::GFP strain, supporting the conclusion that this GFP tag strain is not immunologically inert and therefore, can be used in immunological assays.

Monocytes can differentiate into either macrophages or dendritic cells, whose three main functions are phagocytosis, antigen presentation and cytokine production. (146). These cell types, together with neutrophils and mast cells are recognized to function as professional phagocytes (147). *S. brasiliensis* pGAPDH::GFP yeasts (cytosolic GFP expression), were used to analyse phagocytosis and, like other studies, the GFP fluorescence was intense enough to be visible after phagocytosis both in the microscopic and FACS analysis (138,148–150).

Few articles have reported the phagocytosis index while using *S. brasiliensis*. Ferreira's work (109) obtained percentages of phagocytosis ranging from 70 to 90% while using the MOI (hMDM:fungi) of 1:3 and an incubation period of 2 hours. Our experiments used the MOI of 1:5 and found a lower phagocytosis percentage of 64.25 ± 9.96%. In Rossato's experiments (77,78), when using BMDMs at 3h of incubation and an MOI of 1:5, the phagocytosis index was on average 70%, but the method used to count the inoculum was not clarified. These differences in the phagocytosis index might be caused by divergent Neubauer chamber counting methodologies. In the Neubauer chamber, the strategy for our work was to count each cell individually, despite any cell cluster. Since another possible methodology is to consider cell clusters as single counts, the resulting divergent inoculum concentration can difficult comparison between phagocytosis indexes.

Concluding, from the two strains tested, only the pGAPDH::GFP *S. brasiliensis* strain proved to be useful in infection assays of monocytes/macrophages. Its cytoplasm GFP expression allowed a strong fluorescence visualization inside monocytes/macrophages, in both microscopic and FACS analysis. The pGAPDH::H2A::GFP *S. brasiliensis* strain, however, failed to provide a correlation between loss of cell viability or cell death and loss of GFP fluorescence, and its GFP fluorescence was not visible upon monocytes/macrophages engulfment.

CHAPTER 5

Discussion and Future prospects

Sporotrichosis is the most prevalent subcutaneous mycosis worldwide and has become a public health concern that will likely worsen in the future (Rodrigues et al., 2020). The etiologic agents of this disease are fungi often present in the pathogenic clade of the Sporothrix genus, inside the Ophiostomatales order, but some cases can be caused by the environmental clade, associated with the sapronoses form of sporotrichosis (1,3,16). Among the Sporothrix genus, *S. brasiliensis* is reported the most virulent, exhibiting the worst clinical manifestations (4,5). Infection mechanisms and virulence factors of *Sporothrix* organisms are not completely understood, while antifungal resistance reports and zoonoses cases are rising (7,151). For decades until the mid-1990s, feline sporotrichosis in Brazil appeared only as sporadic, self-limiting clusters. However, over the last decades in Brazil, the sporotrichosis epidemiological scenario changed drastically and became the most endemic country in the world (Rodrigues et al., 2020; Y Zhang et al., 2015). Rio de Janeiro state in is the greatest feline zoonotic transmission epicentre, with more than 4,000 human and 4,000 feline diagnosed cases (Isabella D F Gremião et al., 2015). Similar epidemics also are occurring in São Paulo and Rio Grande do Sul states, with a high prevalence of S. brasiliensis infections (Rodrigues et al., 2016). Cats play an important role in the S. brasiliensis infection, due to their susceptibility to sporotrichosis and highly transmissibility to both felines and humans (Lloret et al., 2013; Y Zhang et al., 2015). Despite the increasing incidence of sporotrichosis, it is unclear which virulence traits are involved in the establishment, development, and severity of this disease. Therefore, in the long term we aim to contribute for the better understanding of this mycosis and *S. brasiliensis* virulence mechanisms.

A widely used methodology to unravel virulence mechanisms for organism is the generation of mutant libraries that allow posterior studies of genes function (152). The genetic manipulation of thermodimorphic fungi is challenging due to the occurrence of non-legitimate recombination. However, genetic manipulation of thermodimorphic fungi have already been stablished through successful ATMT protocols, including *Sporothrix* spp. (98,103,109,153). Part of our work is an extension of Ferreira's thesis (109), further optimizing the ATMT protocol for the *S. brasiliensis* species (Chapter 3), which can provide a mutant library to help uncover associations between gene functions and virulence traits of this emerging and highly virulent pathogen. We managed to produce mutants using three different *S. brasiliensis* strains. The ideal co-cultivation conditions for maximum transformation rates were 72h of co-cultivation at 26°C while using the AGL-1 strain at ratio of 2 bacteria to 1 yeast cell. In these conditions, we obtained 3179 ± 1171 transformants/co-cultivation.

The exact role of immune cells in Sporothrix infection is not yet fully elucidated. Still, macrophages are probably the most important immune cells for containing and terminating sporotrichosis (68,69) since

phagocytic activity plays a crucial role in the surveillance and clearance of fungal pathogens (70,71). With optimized ATMT protocol for *S. brasiliensis*, our group in the laboratory managed to produce strains that express GFP in the nucleus (pGAPDH::H2A::GFP) and the cytoplasm (GAPDH::GFP), to perform several fungicidal and phagocytosis experiments, respectively (Chapter 4). Phagocytosis protocols were inspired by Ferreira's in vitro models (109).

Our results using the pGAPDH::H2A::GFP *S. brasiliensis* strain in cell death assays, such as ultraviolet radiation, incubation with high temperatures, and macrophage-fungicidal, showed no correlation between the loss of cell viability and the loss of GFP fluorescence, as reported before (144). However, some authors managed to correlate the percentage mean GFP intensity lost with cell viability markers instead of the binary approach used in the gating strategy of the FACS in this thesis (133,134). Perhaps, future experiments further correlating pGAPDH::H2A::GFP MFI-loss with cell viability markers could also show the same result. Furthermore, upon phagocyte's engulfment, the GFP intensity of the pGAPDH::H2A::GFP cells became indistinguishable from macrophages/monocytes autofluorescence. These results make both phagocytosis and fungal death count not viable for this strain without the use of external stains.

The GAPDH::GFP mutant proved to be a helpful tool for analysing phagocytosis *in vitro*. Like other studies with several microorganisms, the GFP expression from this mutant was intense enough to be visible after phagocytosis, both during the microscopic and FACS analysis (138,148–150). The phagocytosis index was, on average, 59.13 ± 7.01, a bit lower than Ferreira's work (109), which divergent Neubauer chamber counting methodologies might cause.

In conclusion, the ATMT protocol for S. brasiliensis was further optimized, allowing the creation of several mutants expressing fluorescent proteins. From these, two mutants were tested. The GAPDH::GFP *S. brasiliensis* mutant proved to be useful in infection assays of monocytes/macrophages. Its cytoplasm GFP expression allowed a strong fluorescence visualization inside monocytes/macrophages, visible in microscopic and FACS analyses. The pGAPDH::H2A::GFP *S. brasiliensis* mutant failed to provide a correlation between loss of cell viability or cell death and loss of GFP fluorescence, and its GFP fluorescence was not visible upon monocytes/macrophages engulfment.

In the future, we intend to further transform fluorescent tag strains with mutations in their genome that could influence *S. brasiliensis* virulence. Our group has recently performed a dual RNA-sequencing on macrophages infected with *S. brasiliensis* and *S. schenckii* aiming to identify potential virulence factors that provide a competitive advantage to *S. brasiliensis*. This approach has revealed a specific transcriptome signature of *S. brasiliensis* absent in *S. schenckii*, where sialidase-1 was identified on the

top list of the up-regulated genes (upregulation of 700-fold). The creation and characterization of mutants that overexpress or silence sialidase-1 might help explain *S. brasiliensis* increased virulence.

References

1. Rodrigues AM, Della Terra PP, Gremião ID, Pereira SA, Orofino-Costa R, de Camargo ZP. The threat of emerging and re-emerging pathogenic Sporothrix species. Mycopathologia. 2020 Oct;185(5):813–42.
2. Barros MB de L, de Almeida Paes R, Schubach AO. Sporothrix schenckii and Sporotrichosis. Clin Microbiol Rev. 2011 Oct;24(4):633–54.
3. Orofino-Costa R, Macedo PM de, Rodrigues AM, Bernardes-Engemann AR. Sporotrichosis: an update on epidemiology, etiopathogenesis, laboratory and clinical therapeutics. An Bras Dermatol. 2017;92(5):606–20.
4. Arrillaga-Moncrieff I, Capilla J, Mayayo E, Marimon R, Mariné M, Gené J, et al. Different virulence levels of the species of Sporothrix in a murine model. Clin Microbiol Infect. 2009 Jul;15(7):651–5.
5. Rodrigues AM, de Hoog GS, de Camargo ZP. Sporothrix Species Causing Outbreaks in Animals and Humans Driven by Animal–Animal Transmission. PLOS Pathog [Internet]. 2016 Jul 14;12(7):e1005638. Available from: https://doi.org/10.1371/journal.ppat.1005638
6. Alba-Fierro CA, Pérez-Torres A, Toriello C, Romo-Lozano Y, López-Romero E, Ruiz-Baca E. Molecular Components of the Sporothrix schenckii Complex that Induce Immune Response. Curr Microbiol. 2016 Aug;73(2):292–300.
7. Rodrigues AM, de Hoog GS, de Cássia Pires D, Brihante RSN, Sidrim JJ da C, Gadelha MF, et al. Genetic diversity and antifungal susceptibility profiles in causative agents of sporotrichosis. BMC Infect Dis. 2014 Apr;14:219.
8. Gremião IDF, Menezes RC, Schubach TMP, Figueiredo ABF, Cavalcanti MCH, Pereira SA. Feline sporotrichosis: epidemiological and clinical aspects. Med Mycol. 2015 Jan;53(1):15–21.
9. Lloret A, Hartmann K, Pennisi MG, Ferrer L, Addie D, Belák S, et al. Sporotrichosis in cats: ABCD guidelines on prevention and management. J Feline Med Surg. 2013 Jul;15(7):619–23.
10. Zhang Y, Hagen F, Stielow B, Rodrigues AM, Samerpitak K, Zhou X, et al. Phylogeography and evolutionary patterns in Sporothrix spanning more than 14 000 human and animal case reports. Persoonia. 2015 Dec;35:1–20.
11. Schenck B. On refractory subcutaneous abscesses caused by a fungus possibly related to the Sporotricha. Vol. 9. 1898.
12. Queiroz-Telles F, Fahal AH, Falci DR, Caceres DH, Chiller T, Pasqualotto AC. Neglected endemic mycoses. Lancet Infect Dis. 2017 Nov;17(11):e367–77.
13. Silva-Vergara ML, Maneira FRZ, De Oliveira RM, Santos CTB, Etchebehere RM, Adad SJ. Multifocal sporotrichosis with meningeal involvement in a patient with AIDS. Med Mycol. 2005 Mar;43(2):187–90.
14. Hassan K, Turker T, Zangeneh T. Disseminated sporotrichosis in an immunocompetent patient. Vol. 3, Case reports in plastic surgery & hand surgery. 2016. p. 44–7.
15. Montenegro H, Rodrigues AM, Dias MAG, da Silva EA, Bernardi F, de Camargo ZP. Feline sporotrichosis due to Sporothrix brasiliensis: an emerging animal infection in São Paulo, Brazil. BMC Vet Res. 2014 Nov;10:269.
16. Lopes-Bezerra LM, Mora-Montes HM, Zhang Y, Nino-Vega G, Rodrigues AM, de Camargo ZP, et al. Sporotrichosis between 1898 and 2017: The evolution of knowledge on a changeable disease and on emerging etiological agents. Med Mycol. 2018 Apr;56(suppl_1):126–43.
17. Téllez MD, Batista-Duharte A, Portuondo D, Quinello C, Bonne-Hernández R, Carlos IZ. Sporothrix schenckii complex biology: environment and fungal pathogenicity. Microbiology. 2014 Nov;160(Pt 11):2352–65.
18. Fernandes GF, dos Santos PO, Rodrigues AM, Sasaki AA, Burger E, de Camargo ZP. Characterization of virulence profile, protein secretion and immunogenicity of different Sporothrix schenckii sensu stricto isolates compared with S. globosa and S. brasiliensis species. Virulence.

2013 Apr;4(3):241–9.
19. Fernandes GF, Santos PO dos, Amaral CC do, Sasaki AA, Godoy-Martinez P, Camargo ZP de. Characteristics of 151 Brazilian Sporothrix schenckii Isolates from 5 Different Geographic Regions of Brazil: A Forgotten and Re-Emergent Pathogen. Open Mycol J. 2009;3(1):48–58.
20. Rodrigues AM, de Melo Teixeira M, de Hoog GS, Schubach TMP, Pereira SA, Fernandes GF, et al. Phylogenetic analysis reveals a high prevalence of Sporothrix brasiliensis in feline sporotrichosis outbreaks. PLoS Negl Trop Dis. 2013;7(6):e2281.
21. Sasaki AA, Fernandes GF, Rodrigues AM, Lima FM, Marini MM, dos S. Feitosa L, et al. Chromosomal Polymorphism in the Sporothrix schenckii Complex. PLoS One [Internet]. 2014 Jan 23;9(1):e86819. Available from: https://doi.org/10.1371/journal.pone.0086819
22. Zhao M, Zhou X, Liu T, Yang Z. Morphological and physiological comparison of taxa comprising the Sporothrix schenckii complex. J Zhejiang Univ Sci B. 2015 Nov;16(11):940–7.
23. Brilhante RSN, Rodrigues AM, Sidrim JJC, Rocha MFG, Pereira SA, Gremião IDF, et al. In vitro susceptibility of antifungal drugs against Sporothrix brasiliensis recovered from cats with sporotrichosis in Brazil. Med Mycol. 2016 Mar;54(3):275–9.
24. Gremião IDF, Miranda LHM, Reis EG, Rodrigues AM, Pereira SA. Zoonotic Epidemic of Sporotrichosis: Cat to Human Transmission. PLOS Pathog [Internet]. 2017 Jan 19;13(1):e1006077. Available from: https://doi.org/10.1371/journal.ppat.1006077
25. Chakrabarti A, Bonifaz A, Gutierrez-Galhardo MC, Mochizuki T, Li S. Global epidemiology of sporotrichosis. Med Mycol. 2015 Jan;53(1):3–14.
26. Noriega CT, Garay RR, Sabanero G, Basurto RT S-LM. Sporothrix schenckii: cultures in different soils. Rev Latinoam Micol. 1993;35191–194.
27. Madrid IM, Mattei AS, Fernandes CG, Nobre M de O, Meireles MCA. Epidemiological findings and laboratory evaluation of sporotrichosis: a description of 103 cases in cats and dogs in southern Brazil. Mycopathologia. 2012 Apr;173(4):265–73.
28. Oliveira MME, Almeida-Paes R, Gutierrez-Galhardo MC, Zancope-Oliveira RM. Molecular identification of the Sporothrix schenckii complex. Rev Iberoam Micol. 2014;31(1):2–6.
29. Pereira SA, Passos SRL, Silva JN, Gremião IDF, Figueiredo FB, Teixeira JL, et al. Response to azolic antifungal agents for treating feline sporotrichosis. Vet Rec [Internet]. 2010 Mar 1;166(10):290–4. Available from: https://doi.org/10.1136/vr.166.10.290
30. Schubach TMP, Schubach A, Okamoto T, Barros MBL, Figueiredo FB, Cuzzi T, et al. Evaluation of an epidemic of sporotrichosis in cats: 347 cases (1998-2001). J Am Vet Med Assoc. 2004 May;224(10):1623–9.
31. Schwartz IS, Kenyon C, Lehloenya R, Claasens S, Spengane Z, Prozesky H, et al. AIDS-Related Endemic Mycoses in Western Cape, South Africa, and Clinical Mimics: A Cross-Sectional Study of Adults With Advanced HIV and Recent-Onset, Widespread Skin Lesions. Open forum Infect Dis. 2017;4(4):ofx186.
32. Beurmann L, Gougerot H. Les Sporotrichose. Paris: Librairie Felix Alcan. Paris: Librairie Felix Alcan; 1912.
33. Ramos-e-Silva M, Vasconcelos C, Carneiro S, Cestari T. Sporotrichosis. Clin Dermatol. 2007;25(2):181–7.
34. Silva MBT da, Costa MM de M, Torres CC da S, Galhardo MCG, Valle ACF do, Magalhães M de AFM, et al. Esporotricose urbana: epidemia negligenciada no Rio de Janeiro, Brasil. Cad Saude Publica [Internet]. 2012 Oct [cited 2022 Aug 19];28(10):1867–80. Available from: http://www.scielo.br/scielo.php?script=sci_arttext&pid=S0102-311X2012001000006&lng=pt&tlng=pt
35. Barros MBL, Schubach AO, Schubach TMP, Wanke B, Lambert-Passos SR. An epidemic of sporotrichosis in Rio de Janeiro, Brazil: epidemiological aspects of a series of cases. Epidemiol

Infect. 2008 Sep;136(9):1192–6.
36. Gremião IDF, Martins da Silva da Rocha E, Montenegro H, Carneiro AJB, Xavier MO, de Farias MR, et al. Guideline for the management of feline sporotrichosis caused by Sporothrix brasiliensis and literature revision. Brazilian J Microbiol [publication Brazilian Soc Microbiol. 2021 Mar;52(1):107–24.
37. de Miranda LHM, Silva JN, Gremião IDF, Menezes RC, Almeida-Paes R, Dos Reis ÉG, et al. Monitoring Fungal Burden and Viability of Sporothrix spp. in Skin Lesions of Cats for Predicting Antifungal Treatment Response. J fungi (Basel, Switzerland). 2018 Aug;4(3).
38. Chaves AR, de Campos MP, Barros MBL, do Carmo CN, Gremião IDF, Pereira SA, et al. Treatment abandonment in feline sporotrichosis - study of 147 cases. Zoonoses Public Health. 2013 Mar;60(2):149–53.
39. Rosa CS da, Meinerz ARM, Osório LDG, Cleff MB, Meireles MCA. Terapêutica Da Esporotricose: Revisão. Sci Anim Heal. 2018;5(3):212.
40. Pereira SA, Schubach TMP, Gremião IDF, Silva DT da, Figueiredo FB, Assis NV de, et al. Aspectos terapêuticos da esporotricose felina. Acta Sci Vet. 2018 Mar 30;37(4):311.
41. Rodrigues AM, Fernandes GF, Araujo LM, Della Terra PP, dos Santos PO, Pereira SA, et al. Proteomics-Based Characterization of the Humoral Immune Response in Sporotrichosis: Toward Discovery of Potential Diagnostic and Vaccine Antigens. PLoS Negl Trop Dis. 2015;9(8):e0004016.
42. Nascimento RC, Espíndola NM, Castro RA, Teixeira PAC, Penha CVL, Lopes-Bezerra LM, et al. Passive immunization with monoclonal antibody against a 70-kDa putative adhesin of Sporothrix schenckii induces protection in murine sporotrichosis. Vol. 38, European Journal of Immunology. 2008. p. 3080–9.
43. De Almeida JRF, Jannuzzi GP, Kaihami GH, Breda LCD, Ferreira KS, De Almeida SR. An immunoproteomic approach revealing peptides from Sporothrix brasiliensis that induce a cellular immune response in subcutaneous sporotrichosis. Sci Rep [Internet]. 2018 Dec 1 [cited 2022 Aug 19];8(1). Available from: /pmc/articles/PMC5843658/
44. Chen F, Jiang R, Wang Y, Zhu M, Zhang X, Dong S, et al. Recombinant Phage Elicits Protective Immune Response against Systemic S. globosa Infection in Mouse Model. Sci Rep. 2017 Feb;7:42024.
45. Arturo C, Liise-anne P. Accidental Virulence, Cryptic Pathogenesis, Martians, Lost Hosts, and the Pathogenicity of Environmental Microbes. Eukaryot Cell [Internet]. 2007 Dec 1;6(12):2169–74. Available from: https://doi.org/10.1128/EC.00308-07
46. Rossato L, Moreno LF, Jamalian A, Stielow B, de Almeida SR, de Hoog S, et al. Proteins Potentially Involved in Immune Evasion Strategies in Sporothrix brasiliensis Elucidated by Ultra-High-Resolution Mass Spectrometry. mSphere. 2018 Jun;3(3).
47. Arrillaga-Moncrieff I, J C, AM F, F F, Mayayo E. Diferencias en la patogenicidad del complejo de especies Sporothix en un modelo animal. Rev Latinoam Patol [Internet]. 2010;48(2):82–7. Available from: http://scholar.google.com/scholar?hl=en&btnG=Search&q=intitle:No+Title#0
48. Castro RA, Kubitschek-Barreira PH, Teixeira PAC, Sanches GF, Teixeira MM, Quintella LP, et al. Differences in cell morphometry, cell wall topography and gp70 expression correlate with the virulence of Sporothrix brasiliensis clinical isolates. PLoS One. 2013;8(10):e75656.
49. Almeida-Paes R, de Oliveira LC, Oliveira MME, Gutierrez-Galhardo MC, Nosanchuk JD, Zancopé-Oliveira RM. Phenotypic characteristics associated with virulence of clinical isolates from the Sporothrix complex. Biomed Res Int. 2015;2015:212308.
50. Della Terra PP, Rodrigues AM, Fernandes GF, Nishikaku AS, Burger E, de Camargo ZP. Exploring virulence and immunogenicity in the emerging pathogen Sporothrix brasiliensis. PLoS Negl Trop Dis [Internet]. 2017 Aug 30;11(8):e0005903. Available from:

https://doi.org/10.1371/journal.pntd.0005903
51. Silva-Vergara ML, de Camargo ZP, Silva PF, Abdalla MR, Sgarbieri RN, Rodrigues AM, et al. Disseminated Sporothrix brasiliensis infection with endocardial and ocular involvement in an HIV-infected patient. Am J Trop Med Hyg. 2012 Mar;86(3):477–80.
52. Romero-Martinez R, Wheeler M, Guerrero-Plata A, Rico G, Torres-Guerrero H. Biosynthesis and functions of melanin in Sporothrix schenckii. Infect Immun. 2000 Jun;68(6):3696–703.
53. Oliveira MME, Almeida-Paes R, Corrêa-Moreira D, Borba C de M, Menezes RC, Freitas DFS, et al. A case of sporotrichosis caused by different Sporothrix brasiliensis strains: mycological, molecular, and virulence analyses. Mem Inst Oswaldo Cruz. 2019;114:e190260.
54. Teixeira MM, de Almeida LGP, Kubitschek-Barreira P, Alves FL, Kioshima ES, Abadio AKR, et al. Comparative genomics of the major fungal agents of human and animal Sporotrichosis: Sporothrix schenckii and Sporothrix brasiliensis. BMC Genomics. 2014 Oct;15:943.
55. Huang M, Ma Z, Zhou X. Comparative Genomic Data Provide New Insight on the Evolution of Pathogenicity in Sporothrix Species. Front Microbiol. 2020;11:565439.
56. Gauthier GM. Fungal Dimorphism and Virulence: Molecular Mechanisms for Temperature Adaptation, Immune Evasion, and In Vivo Survival. Mediators Inflamm. 2017;2017:8491383.
57. Jacobsen ID, Wilson D, Wächtler B, Brunke S, Naglik JR, Hube B. Candida albicans dimorphism as a therapeutic target. Expert Rev Anti Infect Ther. 2012;10(1):85–93.
58. Camacho E, Niño-Vega GA. Paracoccidioides Spp.: Virulence Factors and Immune-Evasion Strategies. Mediators Inflamm. 2017;2017:5313691.
59. Szymczak WA, Deepe GS, Winters MS. The interface between virulence and host response to the pathogenic fungus Histoplasma capsulatum. Curr Fungal Infect Rep. 2008;2(3):159–64.
60. Liu GY, Nizet V. Color me bad: microbial pigments as virulence factors. Trends Microbiol. 2009 Sep;17(9):406–13.
61. Almeida-Paes R, Borba-Santos LP, Rozental S, Marco S, Zancopé-Oliveira RM, da Cunha MML. Melanin biosynthesis in pathogenic species of Sporothrix. Fungal Biol Rev. 2017;31(1):50–9.
62. Almeida-Paes R, Nosanchuk JD, Zancope-Oliveira RM. Fungal melanins: Biosynthesis and biological functions. Melanin: Biosynthesis, Functions and Health Effects. 2012. 77–107 p.
63. Nosanchuk JD, Casadevall A. The contribution of melanin to microbial pathogenesis. Cell Microbiol. 2003 Apr;5(4):203–23.
64. Song Y, Yao L, Zhen Y, Cui Y, Zhong S, Liu Y, et al. Sporothrix globosa melanin inhibits antigenpresentation by macrophages and enhances deep organ dissemination. Brazilian J Microbiol [publication Brazilian Soc Microbiol. 2021 Mar;52(1):19–31.
65. Marshall JS, Warrington R, Watson W, Kim HL. An introduction to immunology and immunopathology. Allergy, asthma, Clin Immunol Off J Can Soc Allergy Clin Immunol. 2018;14(Suppl 2):49.
66. Ferreira AV, Domiguéz-Andrés J, Netea MG. The Role of Cell Metabolism in Innate Immune Memory. J Innate Immun. 2022;14(1):42–50.
67. Freitas DFS, de Siqueira Hoagland B, do Valle ACF, Fraga BB, de Barros MB, de Oliveira Schubach A, et al. Sporotrichosis in HIV-infected patients: report of 21 cases of endemic sporotrichosis in Rio de Janeiro, Brazil. Med Mycol. 2012 Feb;50(2):170–8.
68. Sassá MF, Ferreira LS, Ribeiro LC de A, Carlos IZ. Immune response against Sporothrix schenckii in TLR-4-deficient mice. Mycopathologia. 2012 Jul;174(1):21–30.
69. Ruiz-Baca E, Pérez-Torres A, Romo-Lozano Y, Cervantes-García D, Alba-Fierro CA, Ventura-Juárez J, et al. The Role of Macrophages in the Host's Defense against Sporothrix schenckii. Pathog (Basel, Switzerland). 2021 Jul;10(7).
70. Aderem A, Underhill DM. MECHANISMS OF PHAGOCYTOSIS IN MACROPHAGES. Annu Rev Immunol [Internet]. 1999 Apr 1;17(1):593–623. Available from:

https://doi.org/10.1146/annurev.immunol.17.1.593
71. Lee WL, Harrison RE, Grinstein S. Phagocytosis by neutrophils. Microbes Infect. 2003 Nov;5(14):1299–306.
72. Jain N, Moeller J, Vogel V. Mechanobiology of Macrophages: How Physical Factors Coregulate Macrophage Plasticity and Phagocytosis. Annu Rev Biomed Eng. 2019 Jun;21:267–97.
73. Meier A, Kirschning CJ, Nikolaus T, Wagner H, Heesemann J, Ebel F. Toll-like receptor (TLR) 2 and TLR4 are essential for Aspergillus-induced activation of murine macrophages. Cell Microbiol. 2003 Aug;5(8):561–70.
74. Netea MG, Sutmuller R, Hermann C, Van der Graaf CAA, Van der Meer JWM, van Krieken JH, et al. Toll-like receptor 2 suppresses immunity against Candida albicans through induction of IL-10 and regulatory T cells. J Immunol. 2004 Mar;172(6):3712–8.
75. Negrini T de C, Ferreira LS, Alegranci P, Arthur RA, Sundfeld PP, Maia DCG, et al. Role of TLR-2 and fungal surface antigens on innate immune response against Sporothrix schenckii. Immunol Invest. 2013;42(1):36–48.
76. Hoving JC. Pneumocystis and interactions with host immune receptors. PLoS Pathog. 2018 Feb;14(2):e1006807.
77. Rossato L, Santos SS Dos, Ferreira LG, de Almeida SR. The importance of Toll-like receptor 4 during experimental Sporothrix brasiliensis infection. Med Mycol. 2019 Jun;57(4):489–95.
78. Rossato L, Silvana Dos Santos S, Ferreira LG, Rogério de Almeida S. The impact of the absence of Toll-like receptor-2 during Sporothrix brasiliensis infection. J Med Microbiol. 2019 Jan;68(1):87–94.
79. Bessa J, Bachmann MF. T Cell-dependent and -Independent IgA Responses: Role of TLR Signalling. Immunol Invest [Internet]. 2010 Jan 1;39(4–5):407–28. Available from: https://doi.org/10.3109/08820131003663357
80. Romani L. Immunity to fungal infections. Nat Rev Immunol. 2011 Apr;11(4):275–88.
81. Nascimento RC, Almeida SR. Humoral immune response against soluble and fractionate antigens in experimental sporotrichosis. FEMS Immunol Med Microbiol. 2005;43(2):241–7.
82. Carlos IZ, Sgarbi DBG, Santos GC, Placeres MCP. Sporothrix schenckii lipid inhibits macrophage phagocytosis: involvement of nitric oxide and tumour necrosis factor-alpha. Scand J Immunol. 2003 Mar;57(3):214–20.
83. de Almeida JRF, Kaihami GH, Jannuzzi GP, de Almeida SR. Therapeutic vaccine using a monoclonal antibody against a 70-kDa glycoprotein in mice infected with highly virulent Sporothrix schenckii and Sporothrix brasiliensis. Med Mycol. 2015 Jan;53(1):42–50.
84. Maia DCG, Gonçalves AC, Ferreira LS, Manente FA, Portuondo DL, Vellosa JCR, et al. Response of Cytokines and Hydrogen Peroxide to Sporothrix schenckii Exoantigen in Systemic Experimental Infection. Mycopathologia. 2016 Apr;181(3–4):207–15.
85. Villalobos-Duno HL, Barreto LA, Alvarez-Aular Á, Mora-Montes HM, Lozoya-Pérez NE, Franco B, et al. Comparison of Cell Wall Polysaccharide Composition and Structure Between Strains of Sporothrix schenckii and Sporothrix brasiliensis. Front Microbiol. 2021;12:726958.
86. Guzman-Beltran S, Perez-Torres A, Coronel-Cruz C, Torres-Guerrero H. Phagocytic receptors on macrophages distinguish between different Sporothrix schenckii morphotypes. Microbes Infect. 2012 Oct;14(12):1093–101.
87. Dale J (Jeremy W., Schantz M von., Plant N. From genes to genomes : concepts and applications of DNA technology [Internet]. 3rd Edition. Wiley-Blackwell; 2012 [cited 2022 Aug 19]. 386 p. Available from: https://www.wiley.com/en-us/From+Genes+to+Genomes%3A+Concepts+and+Applications+of+DNA+Technology%2C+3rd+Edition-p-9780470683866
88. Li D, Tang Y, Lin J, Cai W. Methods for genetic transformation of filamentous fungi. Microb Cell

Fact [Internet]. 2017;16(1):168. Available from: https://doi.org/10.1186/s12934-017-0785-7
89. dos Reis MC, Pelegrinelli Fungaro MH, Delgado Duarte RT, Furlaneto L, Furlaneto MC. Agrobacterium tumefaciens-mediated genetic transformation of the entomopathogenic fungus Beauveria bassiana. J Microbiol Methods. 2004 Aug;58(2):197–202.
90. Smith EF, Townsend CO. A Plant-Tumor of Bacterial Origin. Science (80-) [Internet]. 1907 Apr 26;25(643):671–3. Available from: https://doi.org/10.1126/science.25.643.671
91. De Cleene M, De Ley J. The host range of crown gall. Vol. 42, The Botanical Review. 1976. p. 389–466.
92. Michielse CB, Hooykaas PJJ, van den Hondel CAMJJ, Ram AFJ. Agrobacterium-mediated transformation of the filamentous fungus Aspergillus awamori. Nat Protoc. 2008;3(10):1671–8.
93. Newell CA. Plant transformation technology. Developments and applications. Mol Biotechnol. 2000 Sep;16(1):53–65.
94. Lacroix B, Tzfira T, Vainstein A, Citovsky V. A case of promiscuity: Agrobacterium's endless hunt for new partners. Trends Genet. 2006 Jan;22(1):29–37.
95. Bundock P, den Dulk-Ras A, Beijersbergen A, Hooykaas PJ. Trans-kingdom T-DNA transfer from Agrobacterium tumefaciens to Saccharomyces cerevisiae. EMBO J. 1995 Jul;14(13):3206–14.
96. de Groot MJA, Bundock P, Hooykaas PJJ, Beijersbergen AGM. Agrobacterium tumefaciens-mediated transformation of filamentous fungi. Nat Biotechnol [Internet]. 1998;16(9):839–42. Available from: https://doi.org/10.1038/nbt0998-839
97. Kunik T, Tzfira T, Kapulnik Y, Gafni Y, Dingwall C, Citovsky V. Genetic transformation of HeLa cells by Agrobacterium. Proc Natl Acad Sci U S A. 2001 Feb;98(4):1871–6.
98. Zhang Y, Li G, He D, Yu B, Yokoyama K, Wang L. Efficient insertional mutagenesis system for the dimorphic pathogenic fungus Sporothrix schenckii using Agrobacterium tumefaciens. J Microbiol Methods [Internet]. 2011;84(3):418–22. Available from: http://dx.doi.org/10.1016/j.mimet.2011.01.017
99. Lozoya-Pérez NE, Casas-Flores S, Martínez-Álvarez JA, López-Ramírez LA, Lopes-Bezerra LM, Franco B, et al. Generation of Sporothrix schenckii mutants expressing the green fluorescent protein suitable for the study of host-fungus interactions. Fungal Biol [Internet]. 2018;122(10):1023–30. Available from: https://doi.org/10.1016/j.funbio.2018.07.004
100. Tamez-Castrellón AK, Romo-Lucio R, Martínez-Duncker I, Mora-Montes HM. Generation of a synthetic binary plasmid that confers resistance to nourseothricin for genetic engineering of Sporothrix schenckii. Plasmid [Internet]. 2018;100:1–5. Available from: https://doi.org/10.1016/j.plasmid.2018.09.006
101. Alonso JM, Stepanova AN, Leisse TJ, Kim CJ, Chen H, Shinn P, et al. Genome-wide insertional mutagenesis of Arabidopsis thaliana. Science. 2003 Aug;301(5633):653–7.
102. Sugui JA, Chang YC, Kwon-Chung KJ. Agrobacterium tumefaciens-mediated transformation of Aspergillus fumigatus: an efficient tool for insertional mutagenesis and targeted gene disruption. Appl Environ Microbiol. 2005 Apr;71(4):1798–802.
103. Almeida AJ, Carmona JA, Cunha C, Carvalho A, Rappleye CA, Goldman WE, et al. Towards a molecular genetic system for the pathogenic fungus Paracoccidioides brasiliensis. Fungal Genet Biol. 2007 Dec;44(12):1387–98.
104. Fernandes FF, Oliveira AF, Landgraf TN, Cunha C, Carvalho A, Vendruscolo PE, et al. Impact of Paracoccin Gene Silencing on Paracoccidioides brasiliensis Virulence. MBio. 2017 Jul;8(4).
105. Menino JF, Almeida AJ, Rodrigues F. Gene Knockdown in Paracoccidioides brasiliensis Using Antisense RNA BT - Host-Fungus Interactions: Methods and Protocols. In: Brand AC, MacCallum DM, editors. Totowa, NJ: Humana Press; 2012. p. 187–98. Available from: https://doi.org/10.1007/978-1-61779-539-8_12
106. Wang J-Y, Li H-Y. Agrobacterium tumefaciens-mediated genetic transformation of the

phytopathogenic fungus Penicillium digitatum. J Zhejiang Univ Sci B. 2008 Oct;9(10):823–8.
107. Zemska O, Rappleye CA. Agrobacterium-mediated insertional mutagenesis in Histoplasma capsulatum. Methods Mol Biol. 2012;845:51–66.
108. Gauthier G, Sullivan T, Gallardo S, Brandhorst T, Wymelenberg A, Cuomo C, et al. SREB, a GATA Transcription Factor That Directs Disparate Fates in Blastomyces dermatitidis Including Morphogenesis and Siderophore Biosynthesis. PLoS Pathog. 2010 Apr 1;6:e1000846.
109. Ferreira BH. Sporothrix brasiliensis – From the genome to the phenotype. University of Minho; 2018.
110. Mora-Montes HM, da Silva Dantas A, Trujillo-Esquivel E, de Souza Baptista AR, Lopes-Bezerra LM. Current progress in the biology of members of the Sporothrix schenckii complex following the genomic era. FEMS Yeast Res. 2015;15(6):1–10.
111. Ferreira BH, Ramírez-Prado JH, Neves GWP, Torrado E, Sampaio P, Felipe MSS, et al. Ploidy determination in the pathogenic fungus Sporothrix spp. Front Microbiol. 2019;10(FEB).
112. Martínez-Álvarez JA, García-Carnero LC, Kubitschek-Barreira PH, Lozoya-Pérez NE, Belmonte-Vázquez JL, de Almeida JRF, et al. Analysis of some immunogenic properties of the recombinant Sporothrix schenckii Gp70 expressed in Escherichia coli. Future Microbiol [Internet]. 2019 Mar 1;14(5):397–410. Available from: https://doi.org/10.2217/fmb-2018-0295
113. Jones HD, Doherty A, Wu H. Review of methodologies and a protocol for the Agrobacterium-mediated transformation of wheat. Plant Methods. 2005 Sep;1(1):5.
114. Wang S, Chen H, Wang Y, Pan C, Tang X, Zhang H, et al. Effects of Agrobacterium tumefaciens strain types on the Agrobacterium-mediated transformation efficiency of filamentous fungus Mortierella alpina. Lett Appl Microbiol [Internet]. 2020 May 1;70(5):388–93. Available from: https://doi.org/10.1111/lam.13286
115. Michielse CB, Hooykaas PJJ, van den Hondel CAMJJ, Ram AFJ. Agrobacterium-mediated transformation as a tool for functional genomics in fungi. Curr Genet. 2005;48(1):1–17.
116. Sbaraini N, Tomazett MV, Penteriche AB, Gonçales RA, Camargo M da S, Bailão AM, et al. An efficient Agrobacterium tumefaciens-mediated transformation method for Simplicillium subtropicum (Hypocreales: Cordycipitaceae). Genet Mol Biol. 2021;44(3):e20210073.
117. Lin L, Wang F, Wei D. Chlorimuron ethyl as a new selectable marker for disrupting genes in the insect-pathogenic fungus Metarhizium robertsii. J Microbiol Methods. 2011 Nov;87(2):241–3.
118. Blochlinger K, Diggelmann H. Hygromycin B phosphotransferase as a selectable marker for DNA transfer experiments with higher eucaryotic cells. Mol Cell Biol. 1984 Dec;4(12):2929–31.
119. Larionov A, Krause A, Miller W. A standard curve based method for relative real time PCR data processing. BMC Bioinformatics [Internet]. 2005;6(1):62. Available from: https://doi.org/10.1186/1471-2105-6-62
120. Du Z, Zong Q, Gao H, Guo Q, Liu T, Chen W, et al. Development of an Agrobacterium tumefaciens-mediated transformation system for Tilletia controversa Kühn. J Microbiol Methods [Internet]. 2021;189(March):106313. Available from: https://doi.org/10.1016/j.mimet.2021.106313
121. Koukolíková-Nicola Z, Hohn B. How does the T-DNA of Agrobacterium tumefaciens find its way into the plant cell nucleus? Biochimie. 1993;75(8):635–8.
122. Talhinhas P, Muthumeenakshi S, Martins J, Oliveira H, Sreenivasaprasad S (Prasad). Agrobacterium-Mediated Transformation and Insertional Mutagenesis in Colletotrichum acutatum for Investigating Varied Pathogenicity Lifestyles. Mol Biotechnol. 2008 May 1;39:57–67.
123. Kummasook A, Cooper C, Vanittanakom N. An improved Agrobacterium-mediated transformation system for the functional genetic analysis of Penicillium marneffei. Med Mycol. 2010 May 1;48:1066–74.
124. Figueiredo JG, Goulin EH, Tanaka F, Stringari D, Kava-Cordeiro V, Galli-Terasawa L V, et al. Agrobacterium tumefaciens-mediated transformation of Guignardia citricarpa. J Microbiol Methods

[Internet]. 2010;80(2):143–7. Available from: https://www.sciencedirect.com/science/article/pii/S0167701209003807
125. Orofino-Costa R, de Macedo PM, Bernardes-Engemann AR. Hyperendemia of Sporotrichosis in the Brazilian Southeast: Learning From Clinics and Therapeutics. Curr Fungal Infect Rep [Internet]. 2015;9(4):220–8. Available from: https://www.embase.com/search/results?subaction=viewrecord&id=L605999676&from=export
126. Misteli T, Spector DL. Applications of the green fluorescent protein in cell biology and biotechnology. Nat Biotechnol [Internet]. 1997;15(10):961–4. Available from: https://doi.org/10.1038/nbt1097-961
127. Matz M V, Lukyanov KA, Lukyanov SA. Family of the green fluorescent protein: journey to the end of the rainbow. Bioessays. 2002 Oct;24(10):953–9.
128. Wu L, Yuan Y-W, Jiang X-G, Fu X-L, Lu Z-X, Tu G-H, et al. [Stable green fluorescent protein expression in Toxoplasma gondii mutant]. Zhongguo ji sheng chong xue yu ji sheng chong bing za zhi = Chinese J Parasitol Parasit Dis. 2011 Dec;29(6):439–42.
129. McDevitt JJ, Lees PSJ, Merz WG, Schwab KJ. Use of green fluorescent protein-expressing Aspergillus fumigatus conidia to validate quantitative PCR analysis of air samples collected on filters. J Occup Environ Hyg. 2005 Dec;2(12):633–40.
130. Perez JT, García-Sastre A, Manicassamy B. Insertion of a GFP reporter gene in influenza virus. Curr Protoc Microbiol. 2013;Chapter 15:Unit 15G.4.
131. Sheen J, Hwang S, Niwa Y, Kobayashi H, Galbraith DW. Green-fluorescent protein as a new vital marker in plant cells. Plant J. 1995 Nov;8(5):777–84.
132. Lipták N, Bősze Z, Hiripi L. GFP transgenic animals in biomedical research: a review of potential disadvantages. Physiol Res. 2019 Aug;68(4):525–30.
133. Strebel A, Harr T, Bachmann F, Wernli M, Erb P. Green fluorescent protein as a novel tool to measure apoptosis and necrosis. Cytometry [Internet]. 2001 Feb 1;43(2):126–33. Available from: https://doi.org/10.1002/1097-0320(20010201)43:2%3C126::AID-CYTO1027%3E3.0.CO
134. Steff A-M, Fortin M, Arguin C, Hugo P. Detection of a decrease in green fluorescent protein fluorescence for the monitoring of cell death: An assay amenable to high-throughput screening technologies. Cytometry [Internet]. 2001 Dec 1;45(4):237–43. Available from: https://doi.org/10.1002/1097-0320(20011201)45:4%3C237::AID-CYTO10024%3E3.0.CO
135. Gille C, Spring B, Tewes L, Poets CF, Orlikowsky T. A new method to quantify phagocytosis and intracellular degradation using green fluorescent protein-labeled Escherichia coli: comparison of cord blood macrophages and peripheral blood macrophages of healthy adults. Cytometry A. 2006 Mar;69(3):152–4.
136. Li W, Houston KD, Houston JP. Shifts in the fluorescence lifetime of EGFP during bacterial phagocytosis measured by phase-sensitive flow cytometry. Sci Rep. 2017 Jan;7:40341.
137. Weingart C, Broitman-Maduro G, Dean G, Newman S, Peppler M, Weiss A. Fluorescent Labels Influence Phagocytosis ofBordetella pertussis by Human Neutrophils. Infect Immun [Internet]. 1999 Aug 1;67(8):4264–7. Available from: https://doi.org/10.1128/IAI.67.8.4264-4267.1999
138. Wasylnka JA, Moore MM. Uptake of Aspergillus fumigatus Conidia by phagocytic and nonphagocytic cells in vitro: quantitation using strains expressing green fluorescent protein. Infect Immun. 2002 Jun;70(6):3156–63.
139. den Dulk-Ras A, Hooykaas PJ. Electroporation of Agrobacterium tumefaciens. Methods Mol Biol. 1995;55:63–72.
140. Green Sambrook, Joseph., Sambrook, Joseph., MR. Molecular cloning : a laboratory manual. Cold Spring Harbor, N.Y.: Cold Spring Harbor Laboratory Press; 2012.
141. Kaur H, Nguyen K, Kumar P. Pressure and temperature dependence of fluorescence anisotropy

of green fluorescent protein. RSC Adv. 2022;12(14):8647–55.
142. Mullenders LHF. Solar UV damage to cellular DNA: from mechanisms to biological effects. Photochem Photobiol Sci Off J Eur Photochem Assoc Eur Soc Photobiol. 2018 Dec;17(12):1842–52.
143. Griffiths HR, Mistry P, Herbert KE, Lunec J. Molecular and cellular effects of ultraviolet light-induced genotoxicity. Crit Rev Clin Lab Sci. 1998 Jun;35(3):189–237.
144. Csepregi R, Temesfői V, Poór M, Faust Z, Kőszegi T. Green Fluorescent Protein-Based Viability Assay in a Multiparametric Configuration. Vol. 23, Molecules. 2018.
145. de Vallée A, Bally P, Bruel C, Chandat L, Choquer M, Dieryckx C, et al. A Similar Secretome Disturbance as a Hallmark of Non-pathogenic Botrytis cinerea ATMT-Mutants? Front Microbiol. 2019;10:2829.
146. Germic N, Frangez Z, Yousefi S, Simon H-U. Regulation of the innate immune system by autophagy: monocytes, macrophages, dendritic cells and antigen presentation. Cell Death Differ. 2019 Mar;26(4):715–27.
147. Hünniger K, Kurzai O. Phagocytes as central players in the defence against invasive fungal infection. Semin Cell Dev Biol [Internet]. 2019;89:3–15. Available from: https://www.sciencedirect.com/science/article/pii/S1084952117305402
148. Miura T, Moriya H, Iwai S. Assessing phagotrophy in the mixotrophic ciliate Paramecium bursaria using GFP-expressing yeast cells. FEMS Microbiol Lett. 2017 Jul;364(12).
149. Deeney AS, Maglennon GA, Chapat L, Crussard S, Jolivet E, Rycroft AN. Mycoplasma hyopneumoniae evades phagocytic uptake by porcine alveolar macrophages in vitro. Vet Res. 2019 Jun;50(1):51.
150. Vance J, Santos A, Sadofsky L, Morice A, Cervantes J. Effect of High Glucose on Human Alveolar Macrophage Phenotype and Phagocytosis of Mycobacteria. Lung. 2019 Feb;197(1):89–94.
151. Borba-Santos LP, Rodrigues AM, Gagini TB, Fernandes GF, Castro R, de Camargo ZP, et al. Susceptibility of Sporothrix brasiliensis isolates to amphotericin B, azoles, and terbinafine. Med Mycol [Internet]. 2015 Feb 1;53(2):178–88. Available from: https://doi.org/10.1093/mmy/myu056
152. Alberts B, Johnson A, Lewis J, Raff M, Roberts K, Walter P. Studying gene expression and function. In: Molecular Biology of the Cell. 4th Editio. New York: Garland Science; 2002.
153. Lozoya-Pérez NE, Casas-Flores S, Martínez-Álvarez JA, López-Ramírez LA, Lopes-Bezerra LM, Franco B, et al. Generation of Sporothrix schenckii mutants expressing the green fluorescent protein suitable for the study of host-fungus interactions. Fungal Biol [Internet]. 2018;122(10):1023–30. Available from: https://www.sciencedirect.com/science/article/pii/S1878614618301739